Balance between Filtration and Strength in Porous Structure

Xinxin Su

June 10, 2010

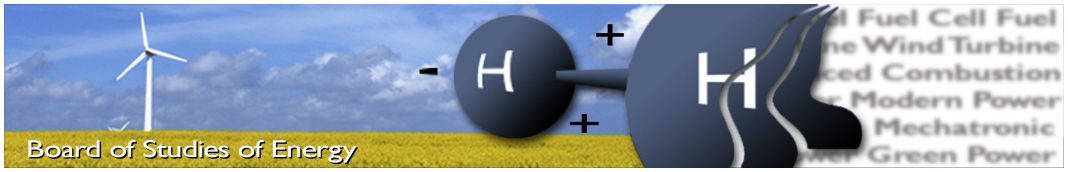

Title:	Balance between Filtration and Strength in Porous Structure
Semester:	10th Semester
Semester theme:	Master thesis
Project period	02.02.2010-08.06.2010
ECTS:	30
Supervisor:	Lasse Rosendahl
Project group:	TEPE4-1040

Xinxin Su

Abstract

Flow through porous filter plate is studied in order to get an understanding of the parameters, thickness and number of rids, influencing the performance of filter. As the alumina is the material used to built-up the filter, and the filter is the core part which affects the performance of the whole filter-pump system obviously. A deeper understanding of the parameter's influence can help us work well enough when we design a filter or the whole filter pump. The LMH of different filter with different parameters are calculated out by hand calculation and the strength of every module is also calculated out from ANSYS simulation. At the end out this thesis, there is a comparison between the hand calculation and CFD simulation. And there is also a comparison with the solid sample, it demonstrated that effective and reasonable creating cavity or channel inside of the porous plate is an important method to increase the permeat.

Preface

This thesis, titled ' Optimization of Filter used in Bio-booster and Dasiy', has been submit to get the Master of Science degreee at Aalborg University of Denmark (AAU). This project is a preparation for my coming job in Dasiy project of Department of Structural and Fluid Mechanics in Grundfos A/S during the period from February 2010 to June 2010, cooresponding to a credit 30 ECTS point.

First of all I want to thank my supervisor Lasse Rosendahl for invaluable guidance and inspiration throught the thesis and heartily help me to coordinate with the other department of university for some unexpected issues. Further I am thankful to my co-supervisor Christian Rasmussen and the rest of the staff at Department of Structural and Fluid Mechanicsfor their technical ideas and support when I came cross some problem. I also acknowledge Grundfos for giving me the chance to work in a opportunity and challege group and work with seasoned engineers. I also have appreciated the help from Jakob Rabjerg Vang when I do the type setting.

Finally, I want to thank all those not mentioned above, but who have helped me in one way or another during my project.

Xinxin Su

Institute of Energy Technology

Aalborg University

8 June 2010

Nomenclature

μ	dynamics vsicosity
$\overrightarrow{v}$	Velocity vector
ρ	Density kg/m^2
σ	normal stress
τ	shear stress
$\triangle E$	potential difference
$\triangle p$	pressure gradient
CS_1	Inlet surface in the normal direction
CS_2	Outlet surface or area in the normal direction
I_z	the moment of inertia for the cross section to the neutral axis
CS	Total surface
EC	equivalent circuit
I	Current A
k	permeability m^2
LMH	The volume flow rate from an unit area and based on an unit pressure difference
M	the bending moment applied on the cross section
n	porosity
p	pressure
Q	volume flow rate
q	Flux m/s
R	resistance
U	volume

Contents

1 Introduction **5**
- 1.1 Applications of Filter . . . 5
  - 1.1.1 Energy . . . 5
  - 1.1.2 Aerospace and Defence . . . 5
  - 1.1.3 Nuclear . . . 5
  - 1.1.4 Food and Beverage . . . 5
  - 1.1.5 Pharmaceutical . . . 6
  - 1.1.6 Water Treatment . . . 6
- 1.2 The Structure of Filter . . . 6
- 1.3 Objective and motivation . . . 7
- 1.4 Outline . . . 8

2 Basic Theory and Considerations **11**
- 2.1 Theory for flowing in porous medium . . . 11
  - 2.1.1 Conservation of Mass-The Continuity Equation . . . 11
  - 2.1.2 Darcy's Law . . . 13
  - 2.1.3 Ohm's Law in porous medium . . . 13
- 2.2 Strength of Ceramic Material . . . 14
  - 2.2.1 Bending Strength . . . 14
    - 2.2.1.1 Normal Stress in Bending . . . 14
    - 2.2.1.2 Shearing Stress in Bending . . . 16
  - 2.2.2 Tensile Strength and Compressive Strength . . . 16
  - 2.2.3 The Maximum Tensile Strength Theory . . . 17

3 Experiments for Porosity and Permeability **19**
- 3.1 Theory used for getting permeability . . . 19
- 3.2 Summary of Membrane Test-bed . . . 20
- 3.3 Experiment Setup . . . 21
- 3.4 Data Processing . . . 22

4 Numerical models and simulations **27**
- 4.1 The First Group Models . . . 27
  - 4.1.1 Geometries compare of solid filter and filter with cavity . . . 27
  - 4.1.2 Pressure boundary conditions . . . 28
  - 4.1.3 Results and Discuss . . . 28
    - 4.1.3.1 Simulations . . . 28

4.1.3.2 Comparsion between Theoretical calculation and Simulation for Cavity Filter . . . 29
4.2 The Cavity Filter with membrane on the top . . . 29
4.2.1 Simulation . . . 30
4.2.2 Theoretical Calculation . . . 30
4.2.3 Comparsion between Simulations and Calculation . . . 33
4.3 Strength Analysis . . . 33

5 Optimization of Filter **37**
5.1 Modularization Analysis of Filter . . . 37
5.1.1 Assumptions . . . 37
5.1.2 Modularization . . . 38
5.2 Function of Filter . . . 40
5.3 Selection of start point . . . 42
5.4 Results from ANSYS . . . 44
5.5 CFD simulation for the best case . . . 44
5.5.1 Result of CFD . . . 47
5.6 On-going CFD . . . 48

Bibliography **53**

A Ansys setip **55**
A.1 Start static structural . . . 55
A.2 Input the Enginnering Data . . . 55
A.3 Import the geometry . . . 56
A.4 Setup . . . 56

B Topology strategy based on GridPro Manual1 **59**
B.1 The first grid . . . 59
B.2 The second grid . . . 60
B.3 Comparison . . . 61

C Step Functions for CFD simulation2 **63**

D Porosity measurement **67**
D.1 Porosity Measurement . . . 67
D.2 Porosity Measurement . . . 67

List of Figures

1.1 Filter-Pump 6
1.2 Filter-Plate 7
1.3 1/8 of One Filter-Plate 8
1.4 Logic diagram for numerical work 9

2.1 Series Resistance 12
2.2 Series Hydraulic Resistance Concept 14
2.3 Shearing Stress and Normal Stress in bending[3] 15
2.4 Pure Bending and Transverse Bending[3] 15
2.5 Section Modulus in Bending 16

3.1 Membrane Test-bed 20
3.2 Diagram of Test-bed 21
3.3 Console of Membrane Tester 22
3.4 Linearship for Kerafol 2mm Core Material 22
3.5 Linearship for ZeRong Sample 23
3.6 Core material EC 24
3.7 Membrane on the top of Core material EC 24
3.8 Structure of membrane 25

4.1 Geometry of Solid Filter 27
4.2 Geometry of Filter with Cavity 28
4.3 The Pressure outside of the Filter 29
4.4 The Pressure Distribution at Plane-ZX for Solid Filter 30
4.5 The Pressure Distribution at Plane-ZX for Cavity Filter 31
4.6 Intersection Surface of Cavity Filter 32
4.7 LMH_Thickness for HC of Cavity Filter 33
4.8 Intersection Surface of Cavity Filter with Membrane 34
4.9 The Maximum Principle Stress for Cavity Filter under work pressure 35
4.10 The Maximum Principle Stress for Cavity Filter under back flush . . 35

5.1 Cross Section of 2_1.5 Filter 38
5.2 39
5.3 Chart for1/Lx 40
5.4 LMH_{real}vary with thickness and number of rids 42
5.5 LMH_{real}vary with thickness and number of rids 43
5.6 The pressure distribution of back flush 45
5.7 The pressure distribution of work state 45

5.8 The relation between pressure and maximum principle stress 46
5.9 The detail of Figure 5.8 46
5.10 The picture of simplified CFD model 47
5.11 Pressure distribution in the xz plane of case1.5_3 48
5.12 The vector in xz Plane 49
5.13 The schematic of On-going CFD 49

A.1 Start static structural 55
A.2 engineering Data 56
A.3 Mechnical Tab 57

B.1 First topology 59
B.2 Detial of First Grid 60
B.3 Second topology and surfaces 60
B.4 The second grid 61

C.1 Cross Section of 1_1.5 Filter 64
C.2 Detail of the filter membrane 64

D.1 Dead-end pores.[4] 68
D.2 Porosimeter based on Boyle Mariotte's law 68

List of Tables

3.1 Detail of Membrane Test-bed 21

4.1 Results from both Simulation and Theoretical Calculation 33

5.1 some data from Figure 5.3 40
5.2 The values of every terms 41
5.3 The values of x and y 43
5.4 Data from ANSYS 44

B.1 Datas of Grids 61

C.1 Field of definitions 65
C.2 Step function for every field of definitions in x direction 65
C.3 Step function for every field of definitions in y direction 65

Chapter 1

Introduction

1.1 Applications of Filter

All kinds of filters with various filtration technologies are applied to the most demanding of environments, such as Energy, Aerospace and Defence, Nuclear, Food and Beverage, Chemical Process,Water Treatment and Life Science markets [5].

1.1.1 Energy

There is a huge demand for a comprehensive range of filtration and separation products in the energy market. Filtration technology is used over a wide range of applications, including gasification and fuel cell technology, clean coal technologies, hydrocarbons and produced water, the distribution of natural gas, conditioning and treatment of fuel oils.

1.1.2 Aerospace and Defence

There are many filters which are used in not only aircraft but also military equipment to keep all systems from contaminants. So it is vital for these filters have high effectiveness. It is essential to meet and exceed guaranteeting safety, cost effective operation, expectations, reliability and long service life to use effective filter, with high performance, in the most demanding situations.

1.1.3 Nuclear

As we all know, there are potential hazards and operational challenges associated wtih environmental emissions and the protection of the workforce wthin the nuclear industry. The filters, within this process, are bearing high temperature, high radioactivity, chemistry etching and high solid loads.

1.1.4 Food and Beverage

Filtration,an economic and safe method, is applied to food and beverage processing to remove impurities and extend the shelf life of many consumable products.

1.1.5 Pharmaceutical

Within pharmaceutical industry, filtration and separation processes are critical. One side, they should ensure products are not only purified enough, but also suitable for consumption. The other side, they also should not only optimize process economics but also prevent loss of valuable product.

1.1.6 Water Treatment

It has become a leading issue to remove contaminants from untreated water, because of environmental concerns and the future water shortage. An effective filtration technology is extremely important to remove eliminate organic, chemical or other debris to supply clean water for drinking, and also the industrial and science markets.

1.2 The Structure of Filter

In this report, we will try to design a filter, made by alumina, which will be used in Filter-Pump of Grundfos. The Filter-Stacks is the red part of the Filter -Pump in Figure1.1. And from Figure 1.2, the shape of filter, from appearance, is a torus with four circular holes which are used for clean water collectting. The detail of filter plate is shown in Figure 1.3, it is 1/8 of one filter plate. From this figure, we can see that there are cavity and channels created inside of filter plate. The cavity can increase the permeation by reducing the thickness of the porous filter plate.

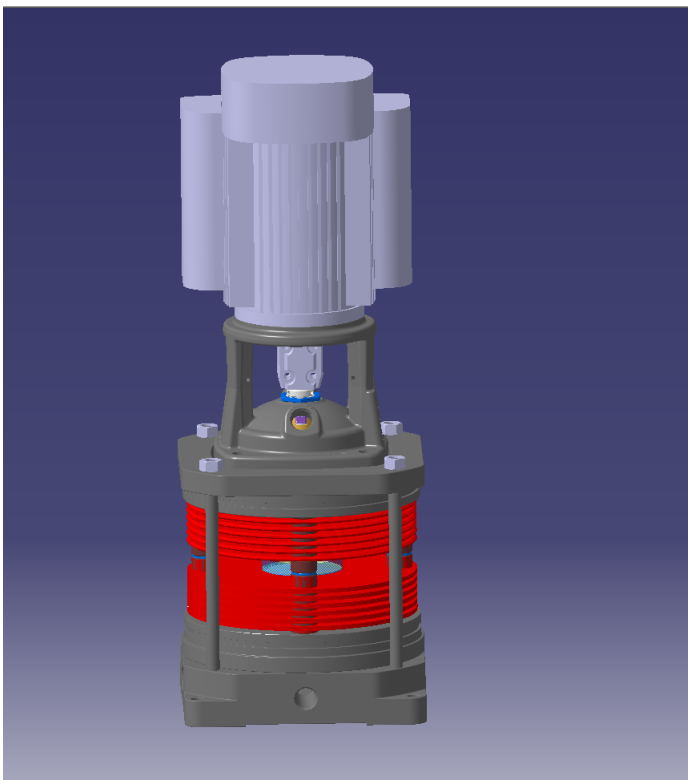

Figure 1.1: Filter-Pump

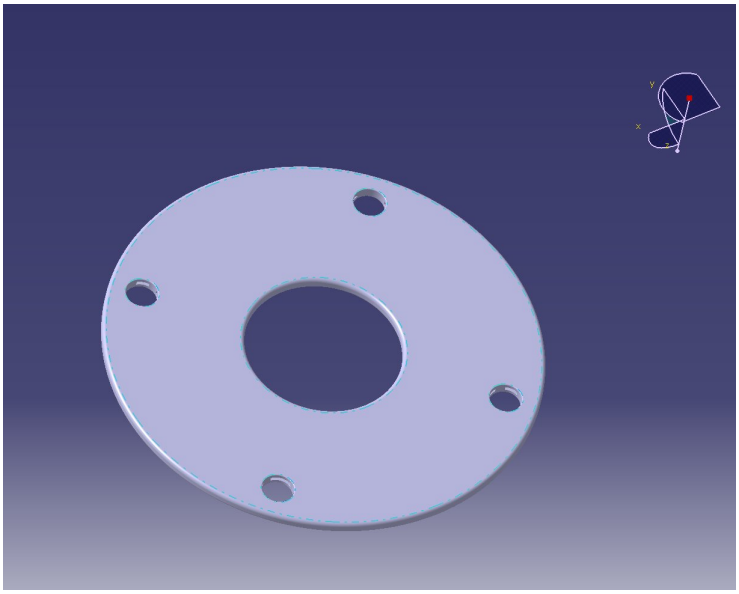

Figure 1.2: Filter-Plate

1.3 Objective and motivation

As Daisy, the new project which focuses on the filter-pump system, is a new project for Grundfos, the knowledge, both the flow in the filter plate and its strength,is still limited. Some preparatory studies have been carried out. However these are far from enough.

The scope of this report has been to continue and extend last semester's work in order to get a good filter plate which has more efficient cross-flow, less pressure loss and 50% more permeat, the water flow through the porous, than before. Both fluid dynamics and mechanical strength of the porous filter plate are related to its parameters such as thickness of shell, geometry of cavity and channel inside of the plate.

The thickness of the filter plate has an effect on both fluid dynamics and mechanical strength. The strength of porous plate can be increased by shell's thickening, but the fluid dynamics, demand cleanliness standards water, is reduced at the same time, vice versa. It is very important to balance the permeation and the strength by choosing a reasonable thickness for the plate shell. In order to increase the permeation, compared with primary porous plate, the creation of cavity, inside of porous plate, is necessary. As has been stated, the geometry of cavity and channel has an effect not only on the permeation, but also on the strength of the porous filter plate. To determine the rough thickness, it is vital to do some theoretical arithmetic and numerical work. For the cavity and channels, the numerical work is the only approach. The geometry will be created by Catia, meshed in GridPro, CFX will be used to calculate the fluid dynamics work and the strength work will be done by ANSYS.

As is known to all, porosity and permeability are two vital parameters when we do some fluid dynamics calculation and computation. These two parameters will be gotten from Membrane Tester, a test-bed in Grundfos.

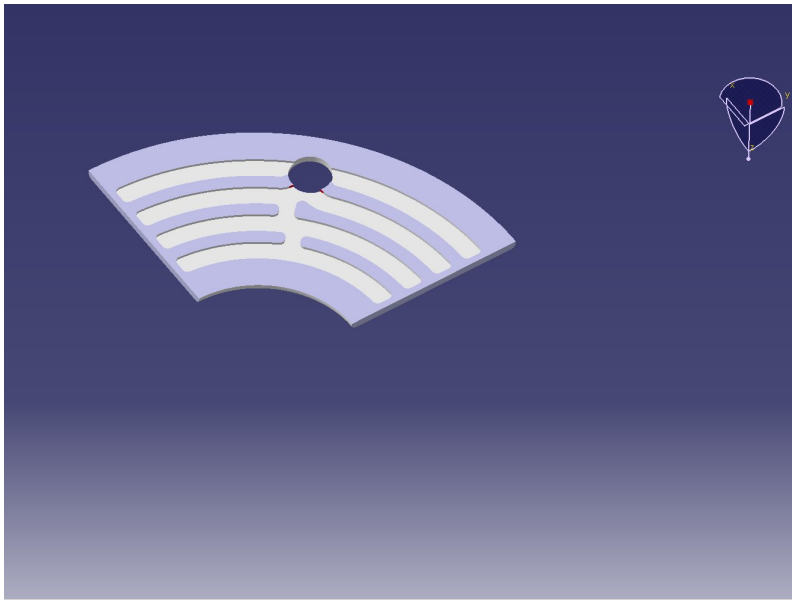

Figure 1.3: 1/8 of One Filter-Plate

1.4 Outline

The work introduced in this report is a selective and important part of my work carried out during my master project, and some basic considerations and simple attempt of numerical work have been left out for clarity.

The chapters contain following:

- Chapter 2:The fundamental governing equations and some theoretical considerations, concerning both the flow inside or outside of a porous media and strength of ceramic, is introduced at the beginning. Some of this chapter's content can be found in several papers, thesises and textbooks is well known by the readers who is familiar with porous media or mechanics of materials.

- Chapter 3: The test process, procedures (which datas could be gotten from which meter and which step), principle and experimental data processing are described in this chapter.

- Chapter 4: In this chapter, mesh information and case setting is introduced, and the numerical models are improved following the flow logic diagram in Figure 1.4. There are three simulations in the chapter, one is solid filter , the second one is a filter with cavity inside. After finish the first two simulation, the will be a comparsion following up to see how much permeat could be increased by creating cavity inside of porous filter. And we also try to get the result by a theoretical calculation based on Darcy's Law, and there is also a comparsion with simulation to see whether this kind of results can beused to check the simulation. The third simulation is adding membrane, $0.085mm$ thickness, on the top of core material and following up is a theoretical calculation use both Darcy's Law and Equivalent Circuit Law. There will be a strength analysis for

the Cavity filter, after CFD simulation and calculations, to check whether this structure is safe, and find out what is the problem.

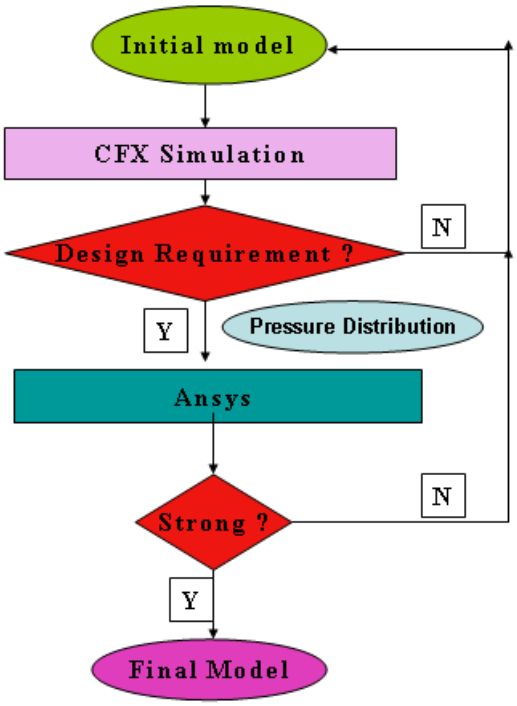

Figure 1.4: Logic diagram for numerical work

- Chapter5:Because CFD simulation is time killer compared with FEA simulation, it is better to find out a good start point based on the hand calculation and the strength simulation. The CFD simulation will set up after the structure gets the safety requirements.
- Chapter6: This report is round off with a conclusion and an outlook.

Chapter 2

Basic Theory and Considerations

In the following the general theory and considerations of this report will be given. This chapter is broken up into two sections, the first one contains some theories and laws for fluid dynamics in porous media. And the second section contains the strength theory about ceramic material.

2.1 Theory for flowing in porous medium

The Continuity Equation and Darcy's Law are the theoretical basis when we calculate the theoretical value of permeation.

2.1.1 Conservation of Mass-The Continuity Equation

The Continuity Equation has both integrated form and differential form, the integrated form is easy to understand and can be used to compute flow in a reasonable time. In this report, we just give the integrated form. Continuity Equation is a mathematical version of Conservation of Mass[6, 4]:

(The mass flow into the control volume in unit time)-(The mass flow out the control volume in unit time)=(The mass increment of the control volume in unit time)

$$-\iint_{CS_1} \rho \overrightarrow{v} \cdot d\overrightarrow{A} - \iint_{CS_2} \rho \overrightarrow{v} \cdot d\overrightarrow{A} = \frac{\partial}{\partial t} \iiint_{CV} \rho d\overrightarrow{V} \tag{2.1}$$

Where $CS_1$and $CS_2$are the flowing into surface and flowing out surface of the control volume respectively. CV is abbreviation of Control volume. ρ is the mass density of fluid, $\overrightarrow{v}$ is the velocity vector of flow. $d\overrightarrow{A}$ is unit area in normal direction, and $d\overrightarrow{V}$is the unit volume in normal direction.

The sum of domains of integration, $CS_1$and CS_2, is the total control surfaceCS, then:

$$-\oiint_{CS} \rho \overrightarrow{v} \cdot d\overrightarrow{A} = \frac{\partial}{\partial t} \iiint_{CV} \rho d\overrightarrow{V} \tag{2.2}$$

This is integrate form of Continuity Equation which is applicable to control volume.

$$\iint_{CS_1} \rho v_{n1} dA - \iint_{CS_2} \rho v_{n2} dA = \frac{\partial}{\partial t} \iiint_{CV} \rho dV \tag{2.3}$$

where v_{n1} is the velocity's projection in the direction which is perpendicular to flowing into surface dA, $v_{n2}$is the velocity's projection in the direction which is perpendicular to flowing out surface dA.

If the fluid is incompressible fluid, because $\rho$is constant, then:

$$\iint_{CS_1} v_{n1} dA = \iint_{CS_2} v_{n2} dA \tag{2.4}$$

Eq. 2.4 explain that the flow, into control volume, equals to the flow, out of control volume, if the fluid is incompressible.

If the flow is one-dimensional steady flow, then:

$$vA = Contant \tag{2.5}$$

or

$$q = \rho vA = Constant \tag{2.6}$$

$$q_1 = q_2 \tag{2.7}$$

where q is the mass flow rate through surface A.

From Eq. 2.7, we can think of series resistance theory, Fig .2.1:

$$I_1 = I_2 = \cdots = I_{n-1} = I_n = \frac{E}{R_1 + R_2 + \cdots + R_{n-1} + R_{1n}} \tag{2.8}$$

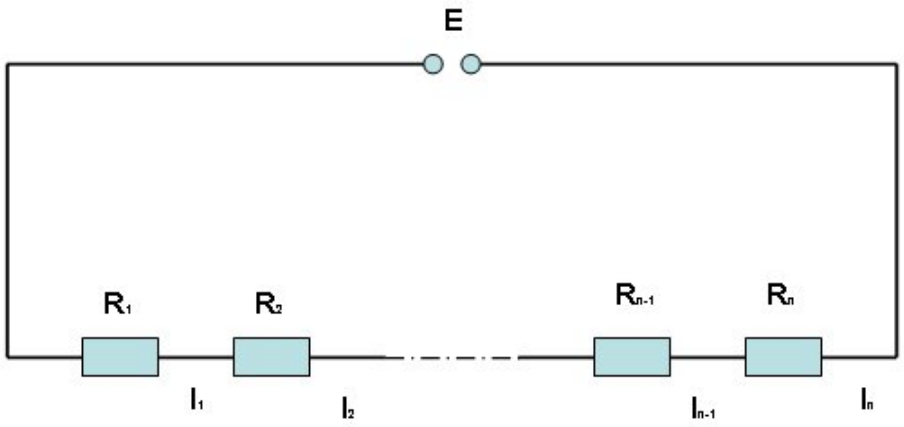

Figure 2.1: Series Resistance

The above two Equations have similar forms.

2.1.2 Darcy's Law

The flow in a porous medium can be divided into four region, pre-Darcy, Darcy, forchheimer and turbulence. If the Reynolds number is in the range from $10^{-5}$to 2.3, then the flow can be descrived by Darcy's Law, which expresses the linearity between the filtration velocity and the pressure difference applied on the porous medium [4, 7, 8]. It was derived from experiments with water through a pipe containing sand by Henry Darcy in 1856, and it is given as

$$q = -\frac{k \cdot \triangle p}{\mu L} \tag{2.9}$$

where q is the filtration flux with a unit m/s, k is the permeability of porous medium with a unit ,μ is dynamic viscosity with a unit $Pa \cdot s$, $\triangle p$ is the pressure difference between the porous plate,$p_{back} - p_{front}$,with a unit Pa, and L is the thickness of porous plate with a unit m.

In membrane technology it is generally assumed that Darcy's Law is applicable in the porous medium. There are some assumptions need to be valid in order to apply Darcy's Law:

- There is no inertial force in the fluid flow.
- The pressure gradient is constant through the porous medium.
- The porous medium, plate, is completely saturated.
- The porous medium is isotropic and the permeability is constant in different directions.
- The fluid is homogeneous which means its density is constant.

2.1.3 Ohm's Law in porous medium

From Eq. 2.9, we can find that if $\frac{k}{\mu L}$ is standed by $R_h$which means hydraulic resistance with a unit $Pa \cdot s/m$, then:

$$q = \frac{-\triangle p}{R_h} \tag{2.10}$$

it is similar with the expression of Ohm's Law:

$$I = \frac{\triangle E}{R} \tag{2.11}$$

where I is electric current with a unit A, $\triangle E$ is the potential difference and R is resistance with a unit Ω.

So when we calculate the filtration velocity through the porous plate with a membrane, showed by Fig.2.2, can be:

$$q = \frac{p_{front} - p_{back}}{R_{hmembrane} + R_{hcore}} \tag{2.12}$$

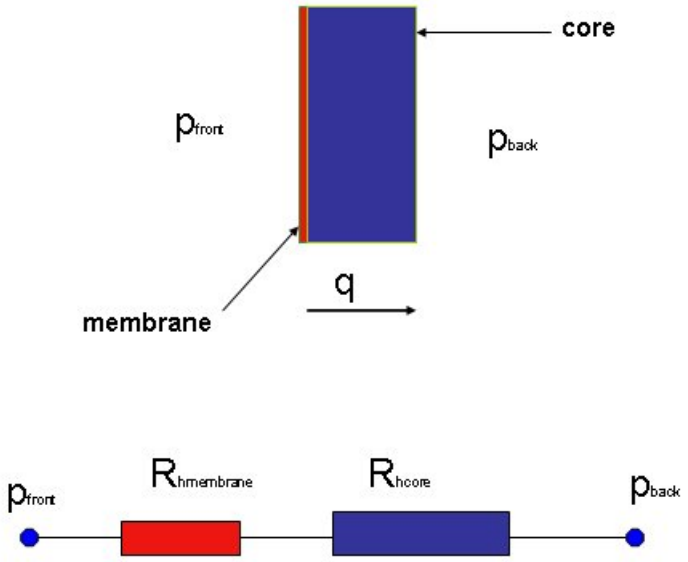

Figure 2.2: Series Hydraulic Resistance Concept

2.2 Strength of Ceramic Material

The same with metals, strength is the basic property of engineering ceramics. The actual strength of ceramics is much lower, two order of magnitude, than its theoretical strength which is demonstrated by a large number of experimental results [9]. In this report, bending strength, tensile strength and compressive strength are the only three strength problem.

2.2.1 Bending Strength

As a general rule, the internal force, applied on the beam, include shear force, F_Q, and bending moment, M. Shear force, which is the sum of tangential and differential internal force τdA, is parallel to the cross section of the beam (Fig. 2.3). τ is shearing stress in bending. M is the integration of σdA in the cross section, and σ is normal stress in bending. If there is no shearing force on any cross section of the beam, the bending is called pure bending (Fig. 2.4). If there is not only shearing force but also bending moment on the cross section, the bending is called transverse bending[3].

2.2.1.1 Normal Stress in Bending

When the bending is pure bending, the normal stress at every point of the cross section :

$$\sigma = \frac{My}{I_z} \tag{2.13}$$

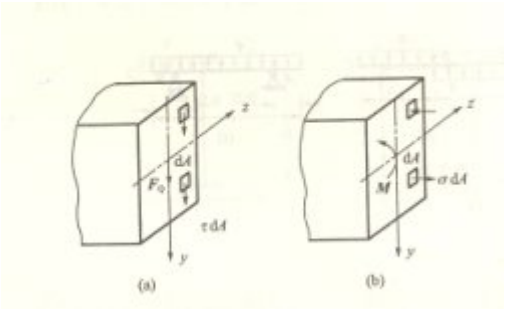

Figure 2.3: Shearing Stress and Normal Stress in bending[3]

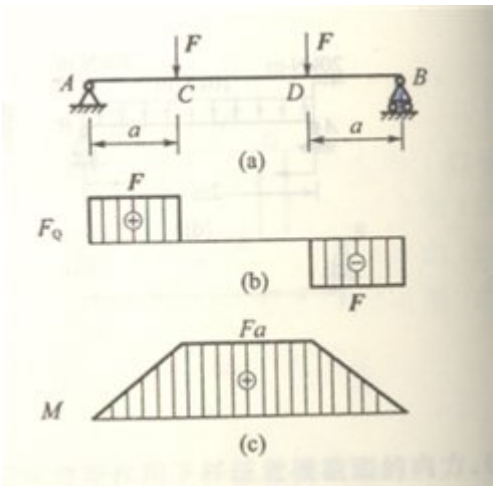

Figure 2.4: Pure Bending and Transverse Bending[3]

Where M is the bending moment applied on the cross section, y is coordinate or the point which is estimated, I_z is the moment of inertia for the cross section to the neutral axis. From Eq. 2.13, it expresses the relationship between y and σ:the higher y the bigger σ. So the maximum normal stress is in the vertical edge where is the farest from the neutral axis.

$$\sigma_{max} = \frac{M}{I_z} y_{max} \tag{2.14}$$

If

$$W_z = \frac{I_z}{y_{max}} \tag{2.15}$$

then:

$$\sigma_{max} = \frac{M}{W_z} \tag{2.16}$$

Where y_{max} is the longest distance to the neutral axis and W_z is section modules in bending. For rectangle (Fig.2.5),

$$W_z = \frac{I_z}{y_{max}} = \frac{bh^3/12}{h/2} = \frac{bh^2}{6} \tag{2.17}$$

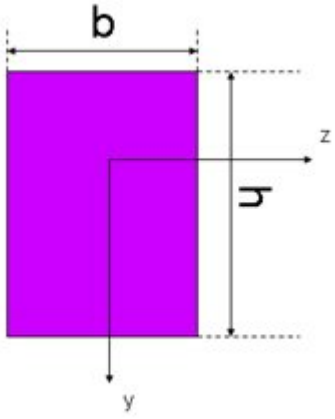

Figure 2.5: Section Modulus in Bending

2.2.1.2 Shearing Stress in Bending

The beam in this report is rectangle cross section beam, so the shearing stress in bending:

$$\tau = \frac{F_Q}{2I_z}(\frac{h^2}{4} - y^2) \tag{2.18}$$

From Eq. 2.18, the distribution of shearing stress in bending along the height of cross section is paraboic distribution. Then :

where $y = \pm h/2$(vertical edge), $\tau = 0$

where $y = 0$(the neutral axis), the shearing stress in the biggest one τ_{max}:

$$\tau_{max} = \frac{F_Q h^2}{8I_z} = \frac{F_Q h^2}{8bh^3/12} = \frac{3}{2}\frac{F_Q}{bh}$$

$$\tau_{max} = \frac{3}{2}\frac{F_Q}{A} \tag{2.19}$$

where $A = bh$, is the area of rectangle cross section [3].

2.2.2 Tensile Strength and Compressive Strength

Tensile strength is the strength criterium when we design ceramic component. Bending strength is 20% to 40% higher than tensile strength. Compressive strength of ceramic material is much greater than its tensile strength, the former is tenfold of the latter.Different extending behavior under these two different load is the reason why there is a strikingly different between tensile strength and compressive strength. When there is a tensile load applied on the ceramic material, the defects in the ceramic material expand fast to fissures; when the load is compression, the broadening speed is very slow and the fissures are connected with each others. Because of this, ceramic materials has a really good performance in compress load. In a word, the tensile strength is the criterium for ceramic component design [9].

2.2.3 The Maximum Tensile Strength Theory

Because the ceramic material is brittle material and tensile strength is not only less than bending strength but also less than compressive strength, the primary cause, leading to non plastic fracture, is maximum tension stress. The material will be broken when one point's maximum tension stress σ_1 gets the ultimate value σ^0[3]. Because the break reason is unconcerned to the state of stress, this ultimate value can be gotten from axial compression. Then the failure condition is:

$$\sigma_1 = \sigma^0 \tag{2.20}$$

When the ultimate value is divided by safety factor, it turns into allowable stress $[\sigma]$, then the strength condition is:

$$\sigma_1 \leq [\sigma] \tag{2.21}$$

As we get the ultimate value for alumina is $35MPa$, the safety factor is chosen as 1.1, so the allowable stress $[\sigma]$ for our filter is $32MPa$.

Chapter 3

Experiments for Porosity and Permeability

Most porous medium have a too complex solid matrix to be described in an exact manner. Nevertheless, the porous medium is recognized as a continum, in which the hydraulic resistance is described by the properties of both the fluid and the solid matrix. Analogy with Ohm's law from circulity, the conductivity of porous medium is denoted the permeability k . The permeability of a porous medium is used to present how good is the conductivity of the porous medium, i.e. the higher permeability means the better conductivity of porous medium[10].

3.1 Theory used for getting permeability

In this experiment, the Darcy's law is inverted to get permeability:

$$q = -\frac{k}{\mu}\frac{\triangle p}{L} \tag{3.1}$$

Where $\triangle p$ is the pressure differnece between the front side and back side of the porous plate: $\triangle p = (p_b - p_f)$,p_f is the pressure of the front side and $p_b$is the pressure of back side. Because p_f is higher than p_b and the sign of q is plus, the sign of left-hand, Eq. 3.2, is minus.

$$k = -\frac{q \centerdot \mu \centerdot L}{\triangle p} \tag{3.2}$$

$$k = -\frac{q \centerdot \mu \centerdot L}{(p_b - p_f)} \tag{3.3}$$

If we know the numeriacl values of q, p_f , $p_b$and μ,then we can get the value of k by substituting the front four values into Eq. 3.3. For the value of dynamic viscosity, μ, can be gotten from some handbooks or papers of fluid mechanics[of Structural and Mechanics [11], Bear [4], Sun [6]]. For the rest three, they should be gotten from experiment.

Eq.3.2 can also has another transformation:

$$k = \frac{Q \centerdot \mu \centerdot L}{A \centerdot TMP * (3600 * 1000 * 10^5)} = \frac{LMH \centerdot \mu \centerdot L}{(3600 * 1000 * 10^5)TMP} \tag{3.4}$$

where,Q is the volume flow rate with a unit l/h, $A$is the filtration area with a unit m^2, TMP is the Trans Membrane Pressure with a unit bar and LMH is the $litre$ per m^2per $hour$ with a unit $l/(m^2 \cdot h)$.

3.2 Summary of Membrane Test-bed

As what mentioned before, the pressures both in front of the porous plate and behind of it, p_f and p_b, and the dynamic viscosity, μ, should measured from experiment before getting permeability,k. The test-be, used in this project, is called Membrane Test-bed, in Fig. 3.1, which is built-up by Grundfos Water-lab.

Figure 3.1: Membrane Test-bed

Fig. 3.2, is a sketch diagram of the components of Membrane Test-bed. The detail can be found in Table. 3.1. In this measurement, the Pressure (P_1) sensor, Pressure (P_2) sensor and the Permeate (Q_2) sensor are enough for we getting the data need for Eq. 3.3. the dead-end flow method is applied in the experiment and partial of components are activated when we run the test-bed. The gray water is pumped to flow following the red arrows, out from gray water sink ,flowing through

CREN pump, sensors behind CREN,sample box, Pressure (P_2) sensor, V4 and Flow (Q_2) sensor, finally the clean water flowing into the Clean water sink.

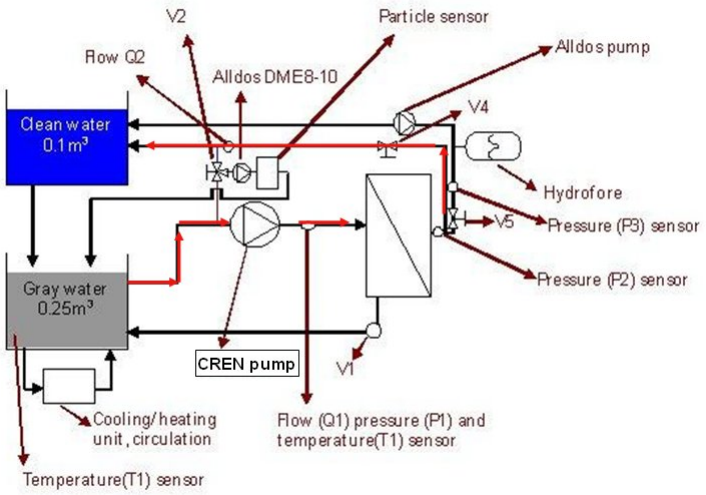

Figure 3.2: Diagram of Test-bed

Flow inlet membrane (Q_1)	0-5001/h (cross flow max. 10m/s with a o.o4cm clearance)
Flow permeate (Q_2)	max 40.01/h at 4bar (flux max $1000l/h/m^2/bar$)
Pressure in front of the plate (P_1)	0-10bar
Pressure behind the plate (P_2)	0-15bar

Table 3.1: Detail of Membrane Test-bed

3.3 Experiment Setup

- Choose the parameters you wanted, and set the pressure at inlet in the PC connected with the Membrane tester.
- Close valve 1 and valve 5, in case the water can flow along the red line.
- Pump gray water into the lower tank and put the chemical agent into the gray water.
- Use heating component to heat the water until its temperature gets $25\,^{\circ}C$ and circulate the gray water in the channels.
- Stop the CREN pump, and open the Pressure box between sensor Q_1 and sensor P_2. Dry the box, and put the sample into it, then seal up it by screws.
- Start the Test bed from console, in Figure 3.3
- After the experiment finished, clean the test bed.

Figure 3.3: Console of Membrane Tester

3.4 Data Processing

For the permeability experiment, we have set up two experiments. The only difference is the test sample, the first one is Kerafol 2mm core material and the second one is zerong sample, a 0.1mm thickness membrane supported by 0.2mm thickness core material. Then we get the linear ships between LMH and TMP, in Figure 3.4 and Figure 3.5.

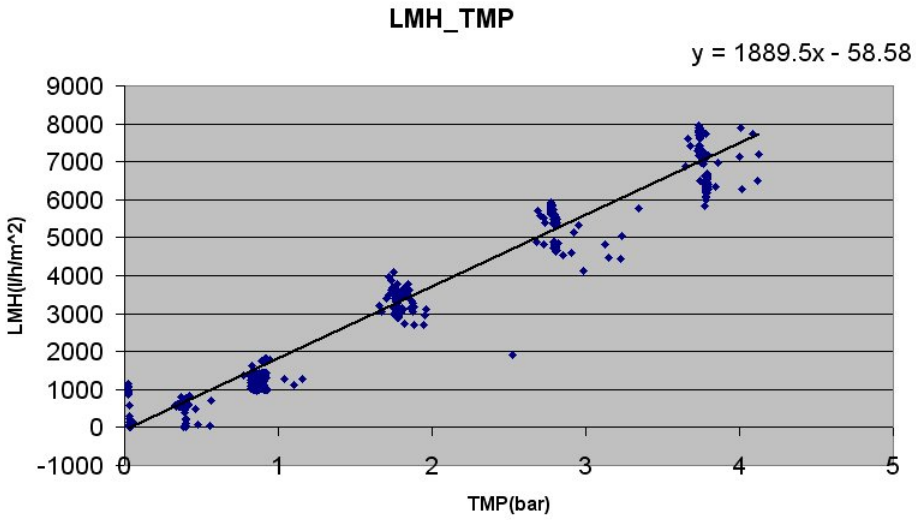

Figure 3.4: Linearship for Kerafol 2mm Core Material

From Figure 3.4, the $\frac{LMH}{TMP}$ is 1889.5, the dynamic viscosity of water in $25\,^{\circ}C$ is 8.9e-4 $Pa\,.\,s$ and the thickness L is $2mm$. Input all the three into Eq.3.4, then we get the permeability of core material is 9.34e-14m^2.

Because the membrane material is really weak, so normally it is not been used all alone, it always needs the core material working as a support. Which means you can not measure the permeability of membrane material, because it is always pasted on the top of core material. As we have stated before at Subsection 2.1.3,we can use equivalent circuit (EC) to simplify this problem:

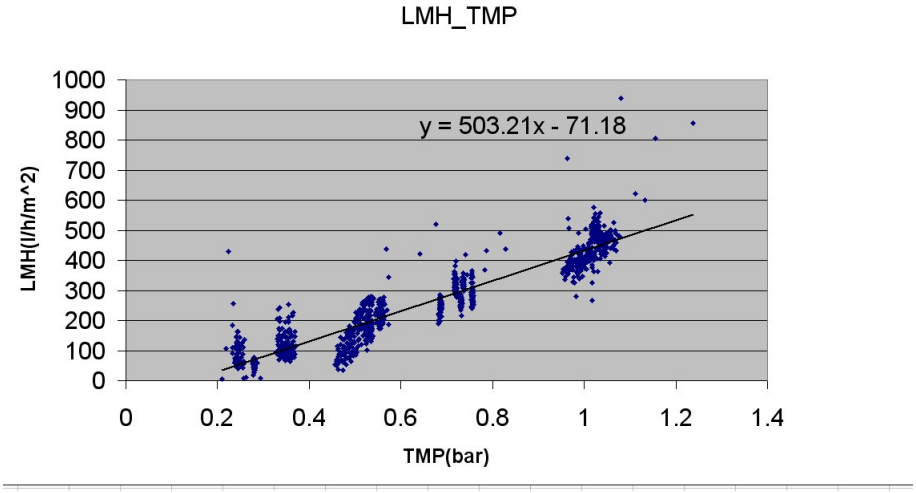

Figure 3.5: Linearship for ZeRong Sample

$$LMH = \frac{Q}{A \cdot \triangle p} = \frac{q_A}{\triangle p} = \frac{k}{\mu \cdot L} \tag{3.5}$$

here the LMH is the linear ship in both Figure 3.4 and Figure 3.5,the flux $q_A$can be regarded as current flow I, the pressure drop $\triangle p$ can be recognized as voltage U, and the count backward of LMH can be recognized as resistance$R$, and from the above equation, we can also find that the LMH, a specific fluid flow through a specific porous medium, only depends on the thickness of the porous medium,and the form of Eq.3.5 can also be transformed by following Eq 3.6:

$$I = \frac{U}{R} \tag{3.6}$$

$$q_A = \frac{\triangle p}{1/LMH} \tag{3.7}$$

The EC for a single resistance, core_material, is shown in Figure 3.6, and the EC for two series resistor, core_material with a membrane on its top, is shown in Figure 3.7. Because:

$$\triangle p_{total} = \triangle p_{membrane} + \triangle p_{core_material} = q_{total} \cdot \frac{1}{LMH_{total}} \tag{3.8}$$

$$\triangle p_{membrane} = q_{membrane} \cdot \frac{1}{LMH_{membrane}} \tag{3.9}$$

$$\triangle p_{core_material} = q_{core_material} \cdot \frac{1}{LMH_{core_material}} \tag{3.10}$$

$$q_{total} = q_{membrane} + q_{core_material}. \tag{3.11}$$

So:

$$\frac{1}{LMH_{total}} = \frac{1}{LMH_{membrane}} + \frac{1}{LMH_{core_material}} \tag{3.12}$$

$$LMH_{membrane} = \frac{LMH_{core_material} \bullet LMH_{total}}{LMH_{core_material} - LMH_{total}} \tag{3.13}$$

As we found the LMH for core_material in Figure 3.4 is 1889.5, and the LMH of the core_material in the second EC should be the same as the first EC.

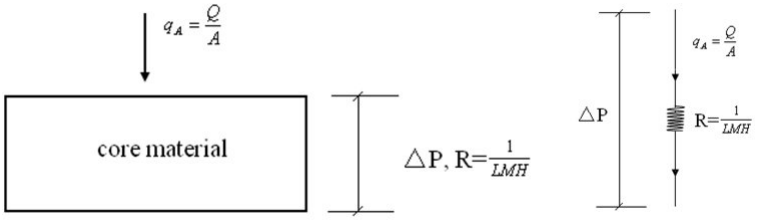

Figure 3.6: Core material EC

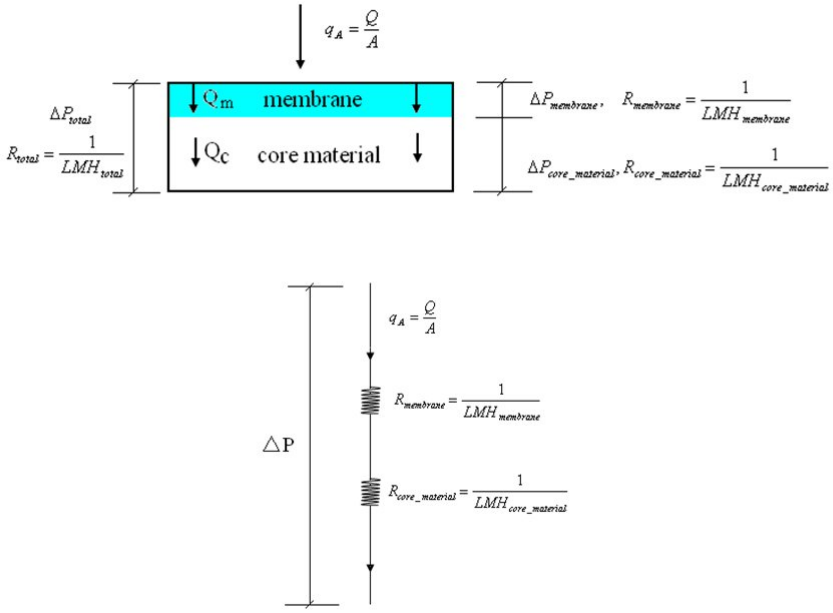

Figure 3.7: Membrane on the top of Core material EC

But we have not gotten enough data for calculate the permeability of membrane, we just know the total LMH and the LMH of core material, there are three unknown quantities, but we just have one equation. So it is necessarily to go on contacting with the supplier to get the exact thickness or get one sample which just has one membrane.

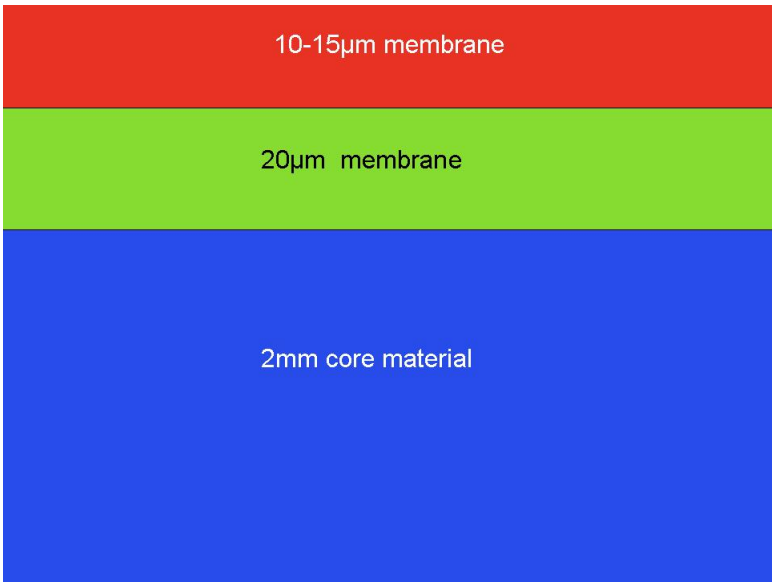

Figure 3.8: Structure of membrane

Chapter 4

Numerical models and simulations

There are three numerical models are developed to describe the flow in porous Alumina-Filters. The front two are models without membrane, and the last one is models with a membrane. The first one is a solid Alumina-Filter 3D model, without membrane, is based on Darcy's Law to describe flow in this kind of filter. The second one is a Alumina-Filter with cavity inside, to compared with the former. There is also an equivalent circuit model to give a rough estimate. The body sections of the last model is totally the same as the second model, the only difference is that there is a membrane on the surface. Both the solid filter and the filter with cavity are analyzed by ANSYS to check their strengths at the end of this chapter.

4.1 The First Group Models

4.1.1 Geometries compare of solid filter and filter with cavity

The geometry of solid filter is very sample, the length of solid filter is $168mm$, its width is $64mm$, and its height is $6mm$ shown in Figure 4.1. The filter with a cavity looks like a $1mm$ thickness shell showed in Figure 4.2.

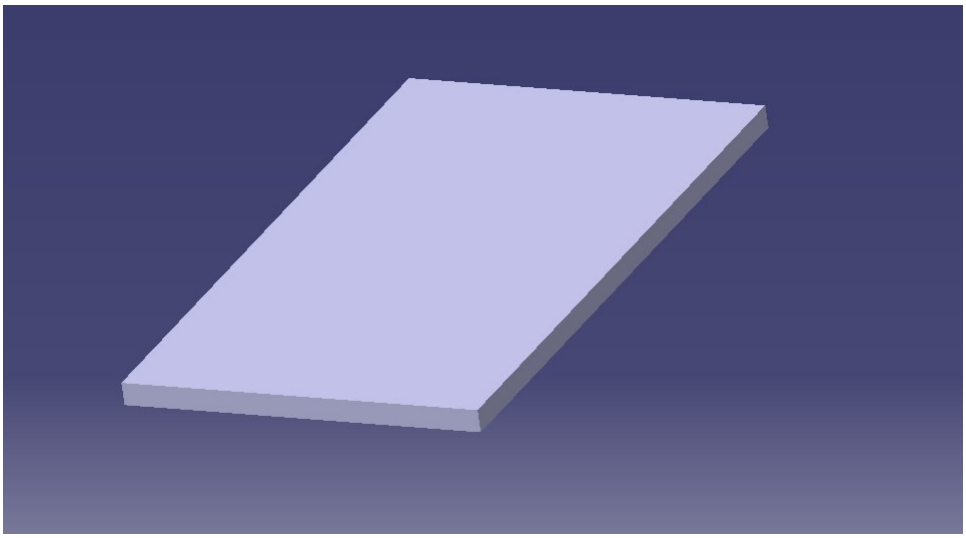

Figure 4.1: Geometry of Solid Filter

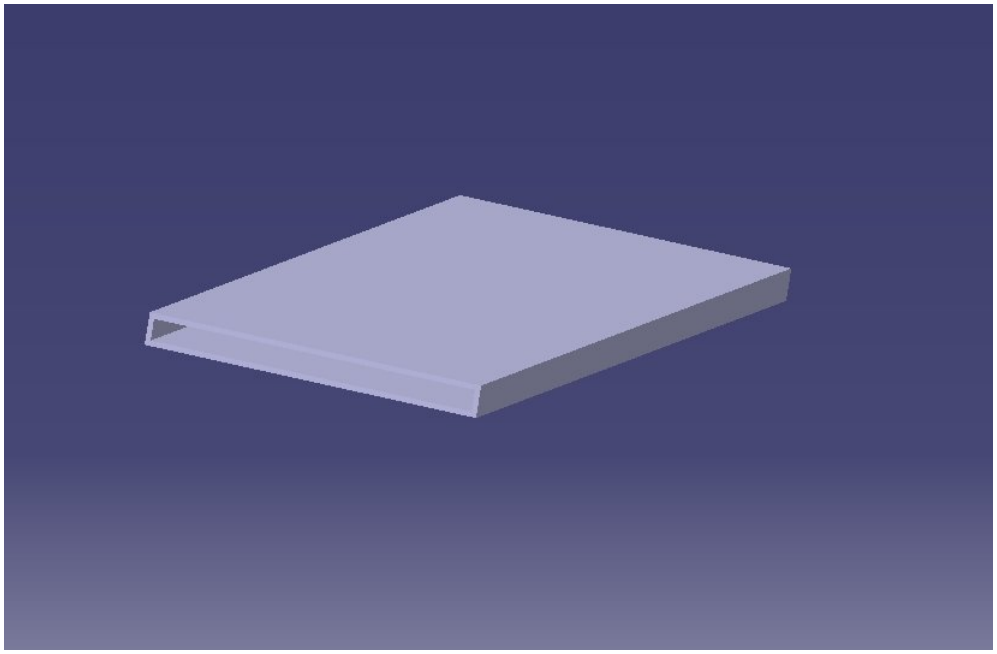

Figure 4.2: Geometry of Filter with Cavity

4.1.2 Pressure boundary conditions

In the physical truth, the pressure outside of the filter is shown in Figure 4.3. When the water flows along the surface of the filter, the pressure near the surface of filter is $2bar$. On the XY plane, the pressure is set as $0Pa$.

4.1.3 Results and Discuss

4.1.3.1 Simulations

After simulation we found that the outflow for the Solid Filter is $2.64m^3/s$, and the outflow for the Cavity Filter is $4.96m^3/s$. The latter is 1.88 times of the former which means the cavity optimization has increased 88% permeat. This result give us a potent reason to create cavity inside the filter. When we get this results, we also want to find the reason why the Solid Filter can not filtrate as much water as the Cavity Filter. From Figure 4.4, we can see that the pressure at the Plane-ZX of Solid Filter is almost 2bar, the confined pressure drop is only in the area near the outlet. This distribution means that most of the filtration surface, for the Solid Filter, is useless. The pressure distribution at Plane-ZX, for Cavity Filter in Figure 4.5, shows that the maximum pressure is $600Pa$ which is along the intersection with wall, and the center area's average pressure is no higher than $420Pa$. The average pressure at Plane-ZX for Solid Filter is $66130Pa$ and the average pressure at Plane-ZX for Cavity Plane is $572Pa$, the latter is 0.865% of the former. To make a long story short, the cavity creation is necessary and obligatory.

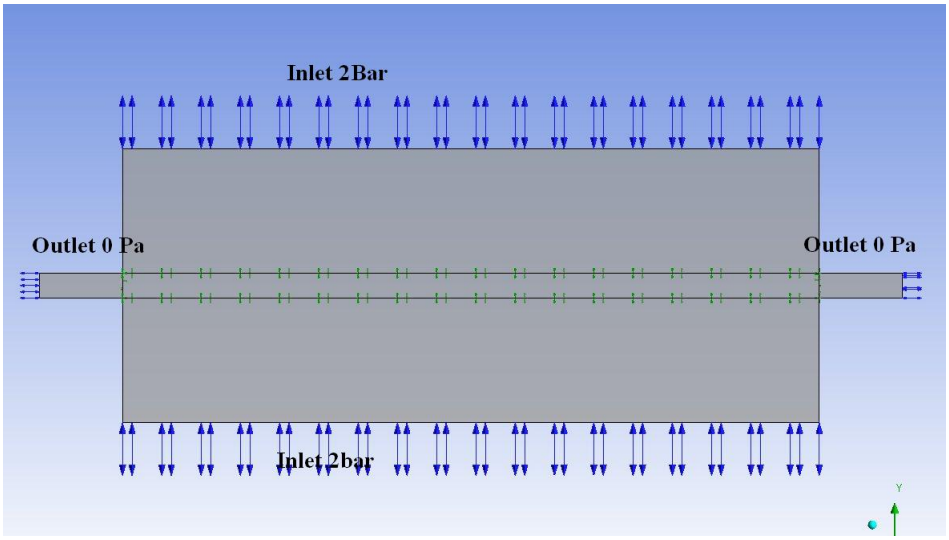

Figure 4.3: The Pressure outside of the Filter

4.1.3.2 Comparsion between Theoretical calculation and Simulation for Cavity Filter

Before we create the geometry of Cavity Filter, we have make a rough theoretical calculation to estimate the performance of the future cavity filter. Before we start the calculation, we have added some assumptions on our model:

- The permeability of rad rectangular areas, area 1 and area 2in Figure 4.6, is ignored and they are recognized as solid wall.
- The porous medium in the dark blue rectangular areas is isotropic.
- The pressure drop along the thickness is constant.
- The pressure inside of the cavity filter is $0Pa$

Based on these assumptions, we have got the variational LMH along with the thicknesses shown in Figure 4.7, it is better to choose $1mm$ as the thickness of the Cavity Filter to get the maximum LMH.The outflow for the hand calculation is 4.85e-$5m^3/s$ compared with simulation result, 4.96e-$5m^3/s$, the difference is no more than 2%. So the hand calculation can give a good expect for the simulation result and it is also the criteria for whether the simulation result is acceptable.

4.2 The Cavity Filter with membrane on the top

After compared with Solid Filter, Cavity Filter is found have a good permeable performance. It should go to next ground estimation to see the performance, permeate and pressure distribution. There is a $0.085mm$ thickness membrane, on the top of the core material,the permeability of which is 1.489e-$16m^2$and its porosity is 0.1. So the geometry of it looks as Figure 4.2, and the intersecting surface is shown in Figure 4.8.

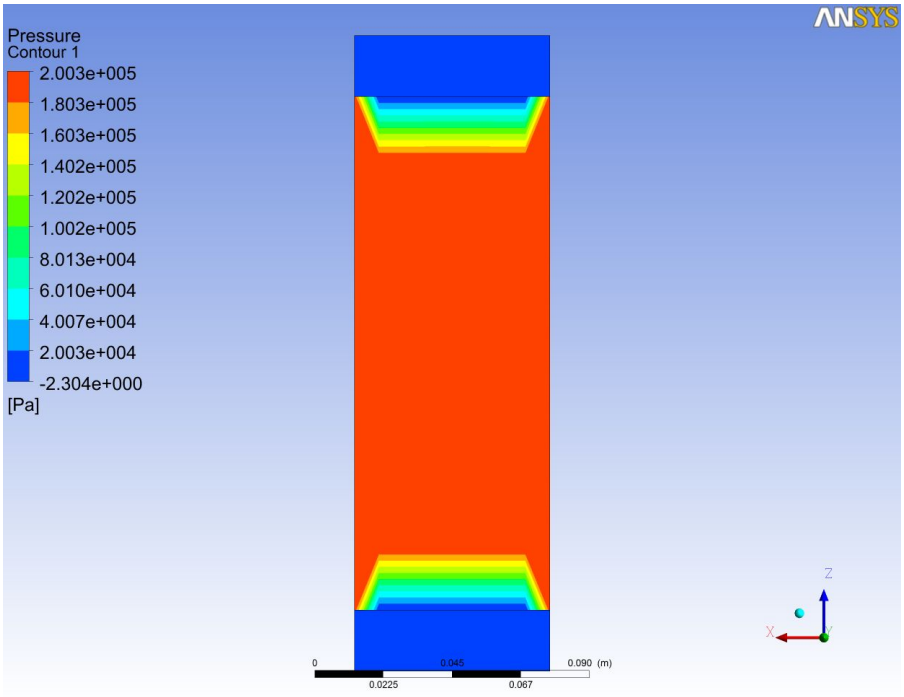

Figure 4.4: The Pressure Distribution at Plane-ZX for Solid Filter

4.2.1 Simulation

The boundary conditions of Cavity Filter with membrane is absolutely the same as the simulation with out membrane, the only difference is in the mesh and thickness part. The top and bottom thickness is increased to $1.085mm$ when it was drawn in Catia, the permeability and porosity of this filter is defined by a step function:

$$k = \begin{cases} 1.489e-16m^2, & -3.085mm \leq y \leq -3mm \\ 1.037e-14m^2, & -3mm < y < 3mm \\ 1.489e-16m^2, & 3mm \leq y \leq 3.085mm \end{cases} \tag{4.1}$$

$$n = \begin{cases} 0.1 & -3.085mm \leq y \leq -3mm \\ 0.4 & -3mm < y < 3mm \\ 0.1 & 3mm \leq y \leq 3.085mm \end{cases} \tag{4.2}$$

In the case, the micro-structural and its extremely tiny grids are avoid. The mesh quality can be kept in an acceptable range. The volume flow rate from simulation is $26.1l/h$, and the LMH is $626l/h/m^2/bar$.

4.2.2 Theoretical Calculation

Before we set up the simulation, we use theoretical calculation to estimate the performance of Cavity Filter with a membrane on its top. There are some assumptions to simplify the calculation:

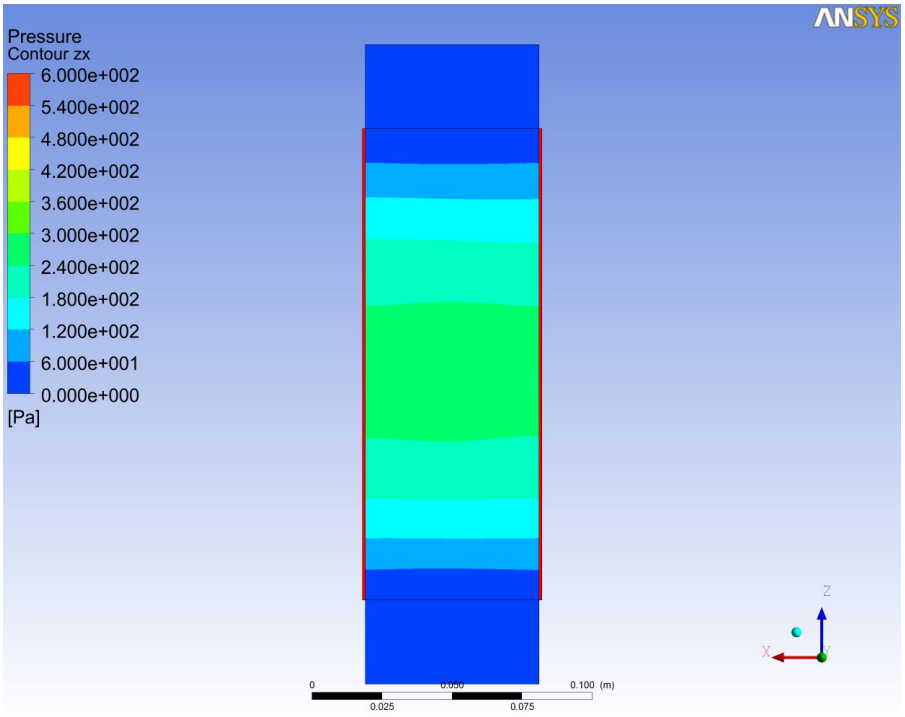

Figure 4.5: The Pressure Distribution at Plane-ZX for Cavity Filter

- The area of red rectangle and membrane on both top and bottom of the red rectangles are recognized as solid wall, which means there is no water flow inside of them.
- The rest area or volume of this filter is isotropic porous medium.
- The pressure drop along the thickness is constant.
- The pressure inside of the cavity is $0Pa$.

Before we start the calculation, we review the equivalent circuit in Figure 3.7,and the voltage is divided by the percentage of how much the resistance take up of the total resistance in the series circuit :

$$\frac{\triangle p_{core_material}}{\triangle p_{membrane}} = \frac{R_{core_material}}{R_{membrane}} = \frac{\frac{1}{LMH_{core_material}}}{\frac{1}{LMH_{membrane}}} \tag{4.3}$$

$$\frac{\triangle p_{core_material}}{\triangle p_{membrane}} = \frac{LMH_{membrane}}{LMH_{core_material}} \tag{4.4}$$

$$LMH = \frac{k}{\mu \cdot L} \tag{4.5}$$

Finally:

$$\frac{\triangle p_{core_material}}{\triangle p_{membrane}} = \frac{k_{membrane} \cdot L_{core_material}}{k_{core_material} \cdot L_{membrane}} \tag{4.6}$$

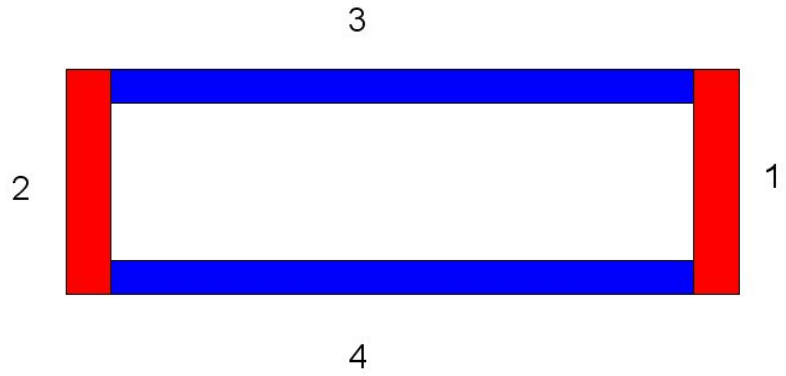

Figure 4.6: Intersection Surface of Cavity Filter

Because:

$$\triangle p_{total} = \triangle p_{membrane} + \triangle p_{core_material} = 2bar \tag{4.7}$$

The trans membrane pressure $\triangle p_{membrane}$is $1.71bar$ and the trans core_material pressure is $0.29bar$. Nearly 85.5% of the total pressure drop is applied on the membrane. Use Darcy's Law2.1.2,w e can get the volume flow rate of this filter Q=$25.2l/h$.

The other one to calculate the volume flow rate is to calculate the LMH_{tatol} first:

As it is mentioned in Eq.3.12

$$\frac{1}{LMH_{total}} = \frac{1}{LMH_{membrane}} + \frac{1}{LMH_{core_material}} \tag{4.8}$$

$$LMH_{total} = \frac{LMH_{core_material} + LMH_{membrane}}{LMH_{membrane} \cdot LMH_{core_material}} \tag{4.9}$$

We can also get LMH by Eq. 3.5:

$$LMH = \frac{k}{\mu \cdot L} \tag{4.10}$$

then:

$$LMH_{total} = \mu \cdot \frac{k_{core_material} \cdot L_{membrane} + k_{membrane} \cdot L_{core_material}}{k_{core_material} \cdot k_{membrane}} \tag{4.11}$$

The total LMH of this filter is 606 $l/h/m^2/bar$, and the volume flow rate of this filter, calculated by this way, is also $25.2l/h$.

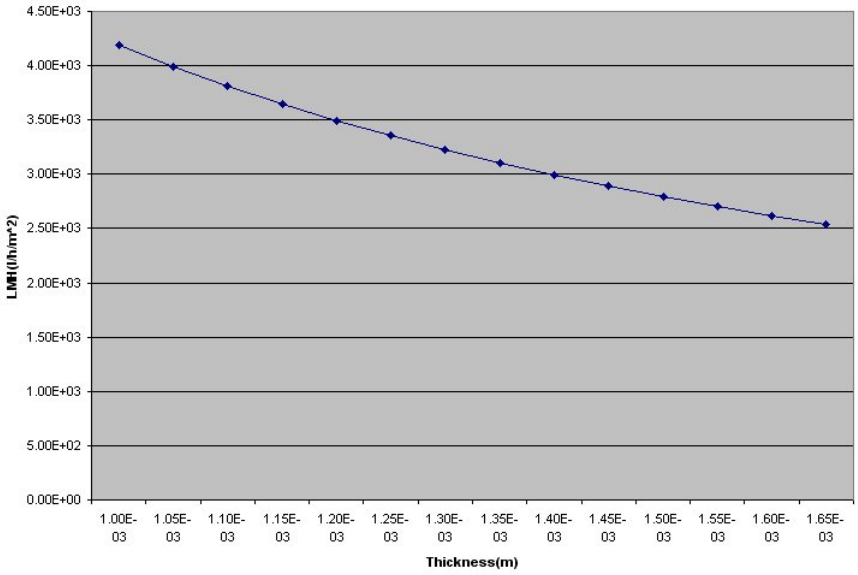

Figure 4.7: LMH_Thickness for HC of Cavity Filter

4.2.3 Comparsion between Simulations and Calculation

Because of the geometry of this filter is symmetrical,so in Table 4.1, we just give the data of Q_U,the volume flow rate from the up side of the filter's interior, and Q_R, the volume flow rate from the right side of the filter's interior. From this table, we can find that the difference between simulation and theoretical calculation is very small, and the theoretical calculation can give a exact expect for the simulation.

	LMH	Q_{Total}(l/h)	Q_U(l/h)	Q_R(l/h)
Simulation Cavity Filter with Membrane	626	26.1	12.7	0.3
Theoretical Calculation	606	25.2	12.6	0
Error(%)	-3.2	-3.15	-0.78	

Table 4.1: Results from both Simulation and Theoretical Calculation

4.3 Strength Analysis

When we design a filter, before its mass production, the strength analysis is indispensable. This subsection will estimate the strength of the Cavity Filter. As we have stated in subsection2.2.3, the the primary cause for the ceramic material, leading to non-plastic fracture, is maximum tension stress. So we just check the

From Figure4.9, we can find that the maximum principle stress is $3.64MPa$ and the tress, over allowable stress, concentrates on two flanks.The maximum principle stress is $3.77MPa$in Figure 4.10, and it is the same as Figure 4.9, the stress over allowable stress concentrates on the two flanks. The difference is that the former's maximum principle stress is outside and the latter's maximum principle stress is inside because of the opposite direction of pressure. And the one vital reason for

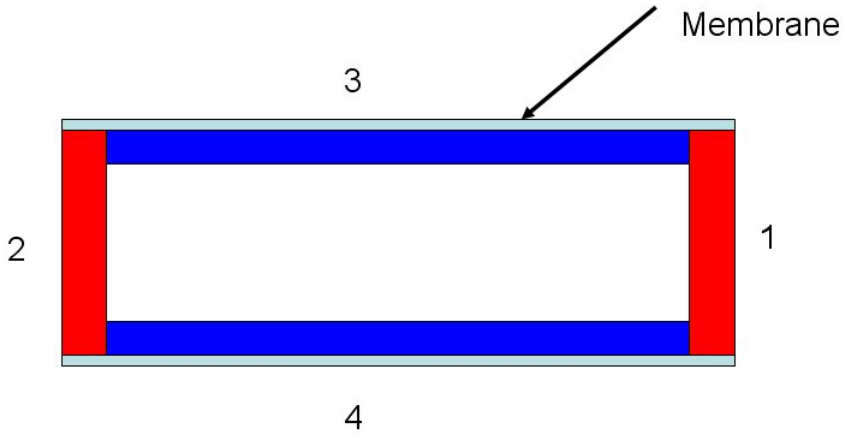

Figure 4.8: Intersection Surface of Cavity Filter with Membrane

the stress concentration is the sharp change of the geometry. In next design, the geometry should avoid sharp change by smoothing.

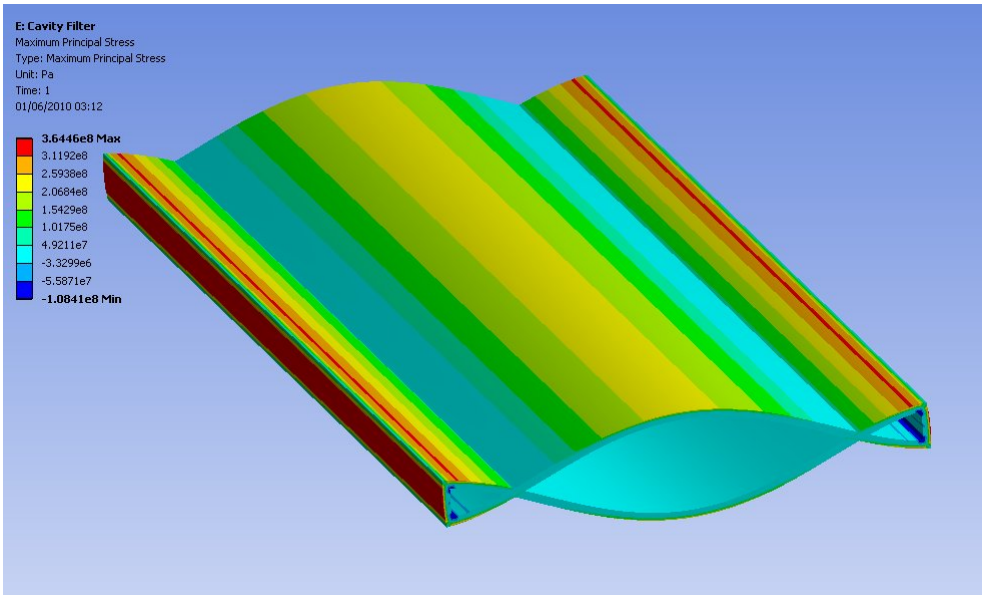

Figure 4.9: The Maximum Principle Stress for Cavity Filter under work pressure

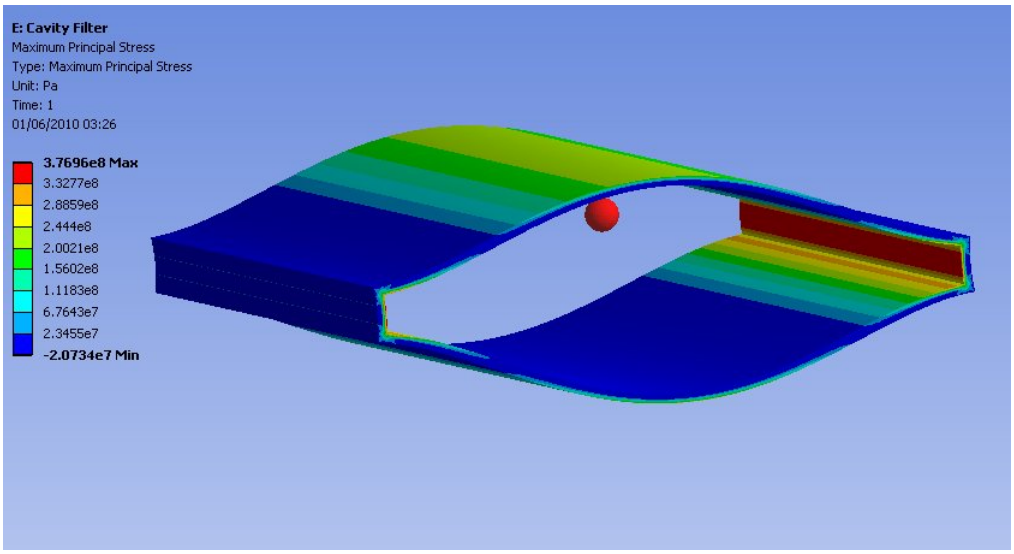

Figure 4.10: The Maximum Principle Stress for Cavity Filter under back flush

Chapter 5

Optimization of Filter

After the comparsions of last chapter, it makes clear that cavities, in side of porous plate, effectively increases the LMH of filter, but in the other side, it also reduces the strength of filter. It is a challenge to find the balance for both strength and LMH. It is not sensible to pay all of your attention to only one side. The bird, which has only one super wing, can not fly. In section 5.1, the filter is disassembled in to many modules by adding some assumptions and the LMH of every module is calculated.In section 5.2, the function between LMH and variable(thickness and number of channels) is set up by adding some assumptions at the end of this chapter. From section 5.3 and section 5.4, the optimal-solution of every type is found out based on the optimization method or law. In section 5.5, the best start point is set up and calculated out, and compared with the hand calculation. In the last section 5.6, the on-going CFD process is described.

5.1 Modularization Analysis of Filter

Because the shape of this filter here is symmetrical, the 3D problem can be simplified into 2D problem. And we also find that the cross sections of these different filters have some same shaped particulars. In order to speed up the hand calculation, it would be best to disassemble one filter into some modules.

5.1.1 Assumptions

There should be some assumptions yo be added so as to disassemble the filter.

- The flow direction is perpendicular with the entrance surface and the flow direction, inside the porous medium, is along the thickness direction which means there is no lateral flow in the porous media.
- The porous medium is isotropic. If it is anisotropic, the permeability may be not constant.
- The pressure gradient along the thickness direction is linear.
- The filter is completely saturated by water.

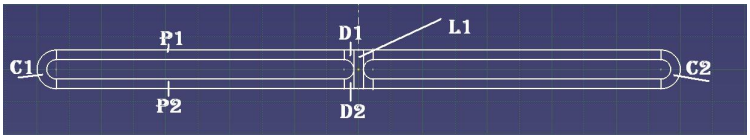

Figure 5.1: Cross Section of 2_1.5 Filter

- There is no flow in the body section of gills, and the flow the permeation in the circular ring area can be recognized as the flow in a plate whose width is the same as the outer girth of this circular ring.
- The pressure,in channel, is $0Pa$, which means the pressure at the outlet surfaces of the porous plate is $0Pa$.
- The pressure distribution outside of the porous plate is constant, which means the pressure at inlets surface of porous plate is $2bar$.

5.1.2 Modularization

Here we just use 2_1.5 filter as an example, this cross section contains all the feature modules. as shown in Figure 5.1 and based on our assumption, there are four module types in a filter, the circular ring(C_1,C_2), the flats($P_1$and P_2), the corner areas($D_1$and D_2) and the useless L_1. All the filters are made up by these four modules , no matter how many channels they have and no matter how much of their thickness.

As we talked in experiment part, the LMH of a flat with membrane has such relationship with its membrane and core:

$$LMH_{flat} = \frac{LMH_{core} \cdot LMH_{membrane}}{LMH_{core} + LMH_{membrane}} \tag{5.1}$$

Because we have assumed that the circular ring can be recognized as a flat, so it also has a LMH:

$$LMH_{cir} = \frac{LMH_{core} \cdot LMH_{membrane}}{LMH_{core} + LMH_{membrane}} \tag{5.2}$$

For the corner area, it is better to have a look at its shape in Figure 5.2, the only problem is the outlet surface or line is not straight but $1/4$ of a ring, so the thickness is not constant. If we assume the right boundary's abscissa is$x = 0$, and the topest of the ring's vertical coordinates is $y = 0$, then there is a function to describe the relationship between x and y:

$$(x + r)^2 + (y + r)^2 = r^2 \tag{5.3}$$

Where r is the radius of circle.
Then the thickness of Area 2 at point x is:

$$L_x = r - \sqrt{r^2 - (x + r)^2} \tag{5.4}$$

Then the flux through Area 2 at point x is:

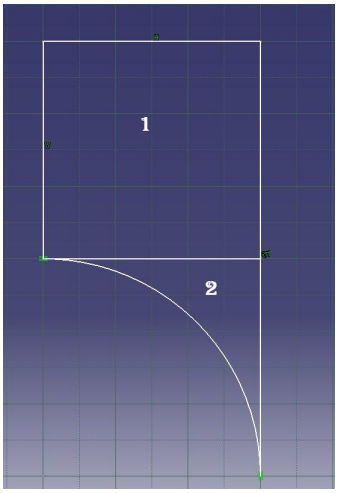

Figure 5.2:

$$q_x = \frac{k \cdot \triangle p}{\mu \cdot L_x} = \frac{k \cdot \triangle p}{\mu \cdot (r - \sqrt{r^2 - (x+r)^2})} \tag{5.5}$$

The volume flow rate through Area 2 is:

$$Q = \frac{k \cdot A \triangle p}{\mu \cdot L_c} = \frac{k \cdot m \cdot \triangle p}{\mu} \int_0^r \frac{dx}{(r - \sqrt{r^2 - (x+r)^2})} \tag{5.6}$$

$$= \frac{k \cdot m \cdot r \triangle p}{\mu \cdot r} \int_0^r \frac{dx}{(r - \sqrt{r^2 - (x+r)^2})} = \frac{k \cdot A \cdot \triangle p}{\mu \cdot r} \int_0^r \frac{dx}{(r - \sqrt{r^2 - (x+r)^2})}$$

where m is the length of filter in Z direction and $L_c$is the characteristic length for Area2 in y direction, $A = m \cdot r$.

$$\frac{1}{L_c} == \frac{1}{r} \int_0^r \frac{dx}{(r - \sqrt{r^2 - (x+r)^2})} \tag{5.7}$$

$$\frac{r}{L_c} == \int_0^r \frac{dx}{(r - \sqrt{r^2 - (x+r)^2})} = \int_0^r \frac{dx}{L_x} \tag{5.8}$$

$$LMH = \frac{Q}{A \cdot \triangle p} = \frac{k}{\mu \cdot L_c} = \frac{k}{\mu \cdot (\frac{L_c}{r})} r \tag{5.9}$$

$\frac{L_c}{r}$ is the reciprocal of areapage between curve and XY-axis 5.3. We have chose three radius,$r_1 = 0.5mm$,$r_2 = 1.0mm$ and the last one $r_3 = 1.5mm$, to plot the $\frac{1}{L_x}$. from the curve, we found that the value of $\frac{1}{L_x}$does not change too much after distance over 0.3mm. So we are very interesting in calculate the area pages of them.

From Table **??**, the most useful information is that the LMH of Area 2 is much higher than what we have gotten before, as the equation 5.12 described before, the LMH of the whole corner area is :

$$\frac{1}{LMH_{total}} = \frac{1}{LMH_{a1_membrane}} + \frac{1}{LMH_{a1_core_material}} + \frac{1}{LMH_{a2}} \tag{5.10}$$

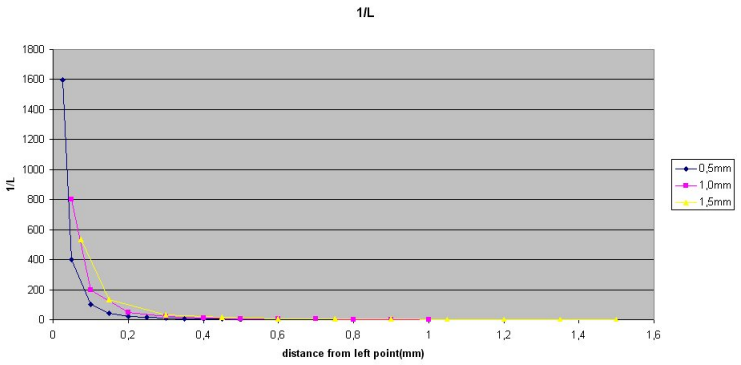

Figure 5.3: Chart for1/Lx

Samples	areapage	$\frac{L_c}{r}$	$LMH \cdot r(l/m/h/bar)$	$LMH(l/m^2/h/bar)$
0.5(mm)	45.3	2.21e-5	1.9e2	3.8e5
1.0(mm)	45.3	2.21e-5	1.9e2	1.9e5
1.5(mm)	45.3	2.21e-5	1.9e2	1.27e5

Table 5.1: some data from Figure 5.3

because $\frac{1}{LMH_{a2}}$ is infinitesimal of higher order, it can should be ignored in case of speeding up the hand calculation. then its form is :

$$\frac{1}{LMH_{total}} = \frac{1}{LMH_{a1_membrane}} + \frac{1}{LMH_{a1_core_material}} \tag{5.11}$$

So the corner module can also be recognized as the porous flat, but the area 2 is cut off. All in all, the LMH of all the modules can be calculated out by Eq 5.12. The whole filter can be opened up work as a porous flat, but the porous area does not equal the area of its surface, it should be the surface area subtracted by the area of gills' cross section which is normal to the flow direction.

5.2 Function of Filter

As we have talked at beginning, there are two direction to optimize a filter. The thickness of the filter is very important in the fluid direction and the number of gills is also very important in the strength direction. As we talked at last subsection, the filtration area is the surface area substrated by the sum of gills' cross section area. If we assume that, the thickness of gills' minimum cross section equals to the thickness of the flat. There should be a function with two variable, the thickness and the amount of gills, can be used in optimum theory to find the best balance of flow and safety.

The ideal LMH of filter is from the Eq. 5.12:

$$\frac{1}{LMH_{total}} = \frac{1}{LMH_{membrane}} + \frac{1}{LMH_{core_material}} \tag{5.12}$$

Then we can do some transformation work:

Terms	m	$k_{core_material}$	$k_{membrane}$	$L_{core_material}$	$L_{membrane}$	μ
Values	6π+184	1.037e-14	1.489e-16	x	0.085	8.9e-4

Table 5.2: The values of every terms

The unit of length is mm, the unit of permeability is m^2, and the unit of velocity is $Pa \cdot s$.

$$\frac{1}{LMH_{ideal}} = \frac{LMH_{core_material} + LMH_{core_material}}{LMH_{membrane} \cdot LMH_{core_material}} \tag{5.13}$$

$$LMH_{ideal} = \frac{LMH_{core_material} \cdot LMH_{core_material}}{LMH_{membrane} + LMH_{core_material}} \tag{5.14}$$

Because:

$$LMH = \frac{k}{\mu \cdot L} \tag{5.15}$$

Then:

$$LMH_{ideal} = \frac{1}{\mu}\left(\frac{k_{core_material} \cdot k_{membrane}}{k_{core_material} \cdot L_{membrane} + k_{membrane} \cdot L_{core_material}}\right) \tag{5.16}$$

The relationship between real LMH and ideal LMH is:

$$LMH_{real} \cdot A_{surface} = LMH_{ideal} \cdot (A_{surface} - A_{Sum-Cross-section}) \tag{5.17}$$

$$LMH_{real} = \frac{A_{surface} - A_{Sum-Cross-section}}{A_{surface}} LMH_{ideal} \tag{5.18}$$

Because the geometry of this filter is symmetrical, and the length in Z-direction is constant. The ratio between areas can be standed by the ratio of circumferences. If M stands for the circumference, then:

$$LMH_{real} = \frac{m - l_{Sum-Cross-section}}{m} LMH_{ideal} \tag{5.19}$$

$$LMH_{real} = \frac{1}{\mu}\frac{m - l_{Sum-Cross-section}}{m}\left(\frac{k_{core_material} \cdot k_{membrane}}{k_{core_material} \cdot L_{membrane} + k_{membrane} \cdot L_{core_material}}\right) \tag{5.20}$$

where $l_{Sum-Cross-section}$ is the sum length of cross section, if we use x ,unit is mm,standing for the thickness and y stand for the number of gills, the values of these terms are shown in Table 5.2.

then, import all the values into the Eq. 5.20:

$$LMH_{real} = \frac{6\pi + 184 - x \cdot (y+2)}{8.9e - 4 \cdot (6\pi + 184)}\left(\frac{1.037e^{-14} \cdot 1.489e^{-16}}{1.0374e \cdot xe^{-3} + 1.489e^{-16} \cdot 8.5e^{-5}}\right) \tag{5.21}$$

The unit of LMH_{real} here is $m^3/s/m^2/Pa$, if you want to transfer the unit to $l/h/m^2/bar$, it should:

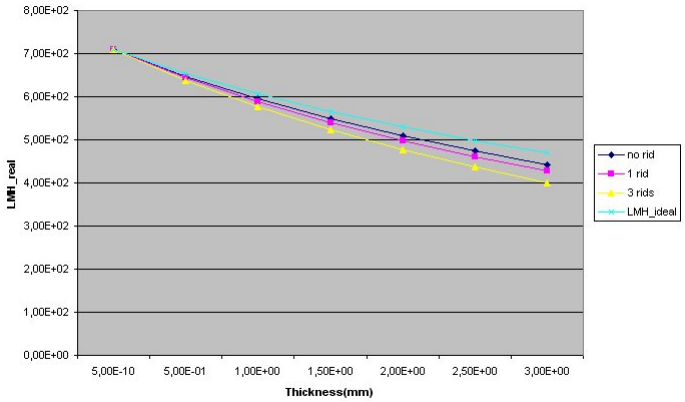

Figure 5.4: LMH_{real}vary with thickness and number of rids

$$LMH_{real} = \frac{6\pi + 184 - x \cdot (y+2)}{8.9e^{-4} \cdot (6\pi + 184)} \left(\frac{1.0374e^{-14} \cdot 1.489e^{-16}}{1.0374e^{-14} \cdot xe^{-3} + 1.489e^{-16} \cdot 8.5e^{-5}} \cdot (3600 \cdot 1000 \cdot 10^5) \right) \tag{5.22}$$

Now we can make curves for LMH of difference thickness and amount of rids(gills) in Figure 5.4 and make the curve of difference compared with theLMH_{ideal} in Figure 5.5. The LMH is decreasing along the thickness's increase, because the increase of thickness reduces $LMH_{core_material}$by refering to equation 5.9, and the first term of right side in equation 5.12 is larger than before, the second term of this equation is constant, then the reciprocal of $LMH_{core_material}$ is increased. It is clear that $LMH_{core_material}$ is decreased. On the other hand, the $LMH_{core_material}$ are also decreasing with the increase of rids' number, that because the increase of rids's number reduces the active area for filtration. These two figures show that anyone of thickness and rids is increased leads to the lower LMH. But it is not that the thinner of thickness and the less of rids are the better for filter design. As we have talked at the beginning of this chapter, the safety requirements need the thickness no less than a certain number and there must be some rids in the filter to support the flats proved by last chapter's strength simulation.

5.3 Selection of start point

In our filter, there are two design variables, thickness and the number of rids. The performance of both fluid portion and strength portion is depended on these two design variable. When we transcribe a verbal statement of the design problem to a mathematical formulation, there are three steps or three aspect should be done [12]:

- The design variables should be identified and defined.
- The cost function should be defined and the expression for it should be developed in terms of variable.
- Develop expression for the identified constrains in terms of design variables.

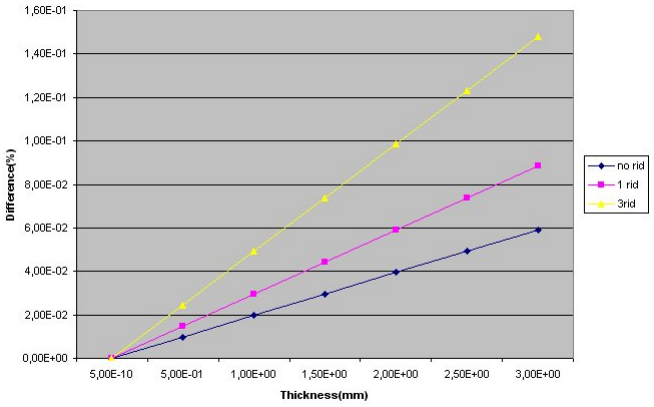

Figure 5.5: LMH_{real}vary with thickness and number of rids

x(mm)	0.5	1.0	1.5	2.0	2.5
y		0		1	3

Table 5.3: The values of x and y

The thickness of the filter pump should be no more than 3 mm, here we set its maximum value is 2.5 mm. Also, it should not be less than 0 mm, hereby its minimum is 0.5 mm. The number of the rids should controlled by this equation,$x(y+2) < 100mm$, but in our filter optimization, there are only three values, 0, 1 and 3, can be used in this problem. And the LMH of the filter should at least 300 $l/h/m^2/bar$, and the maximum principle stress should be no higher than 32 MPa. The design objective is to maximize the LMH of the filter. For the cost function it should be:

$$f(x,y) = -\frac{6\pi + 184 - x\cdot(y+2)}{8.9e^{-4}\cdot(6\pi+184)}\left(\frac{1.0374e^{-14}\cdot 1.489e^{-16}}{1.0374e^{-14}\cdot xe^{-3} + 1.489e^{-16}\cdot 8.5e^{-5}}\cdot(3600\cdot 1000\cdot 10^5)\right) \tag{5.23}$$

The constraint's mathematical forms are:

1. $0.5 \leq x \leq 2.5$
2. $0 \leq y \leq 3$
3. $0 < x \cdot y < 100$

Some constraints can not be transformed into mathematical forms, the maximum stress can not get by hand calculation in this report. The only way get it is by ANSYS simulations.

Use this we give a clear representation for our problem, but we do not want our process inflexible. We do not follow the form of this theory, but we use the idea of it. For the thickness and number of rids are just given some number in Table 5.3. There are three group ANSYS simulations has been set up, the groups are classified by the different numbers of girds. Every group covers all the five thicknesses.

number of rids	0		1		3	
	BF(MPa)	WP(MPa)	BF(MPa)	WP(MPa)	BF(MPa)	WP(MPa)
0.5	6530	5400	9200	9200	183	184
1.0	1030	1000	229	220	51.3	47.6
1.5	555	372	136	92	28.1	17.6
2.0	350	200	81.2	50.2	18.7	10
2.5	286	130	69.8	34.3	1.58	6.59

Here, WP is work pressure and BF is back flush.

Table 5.4: Data from ANSYS

5.4 Results from ANSYS

In order to describe our optimization process clearly, the detail of ANSYS simulations is not say more than is needed. If some information you can not find here, please go to A. Every case's performance under both work pressure and back flush pressure are estimated shown in Table 5.4, and from this table we can found that the maximum principle stress, when the filter pump dong back flush, is higher than the pressure when it is filtrating. That because when the work state is back flush, all the inner surface of the filter is stretched and this side is also thrust surface. In figure 5.6, we can find that the maximum stress happens on the outer rid. the reason is that, the pressure difference on the two side of this rid is the maximum, one side the outer rid need bear the pressure difference, the other side the rid's cross section also need balance the force on the flat. Because of the ratio between rid and flat is obviously very small, the tensile stress on the rid's cross section is much higher than the pressure on the flat. For the work state, the thrust surface is the outer side, and the maximum principle stress happens near the rid, and the stretching is canceled out some by the grid. There are just two cases do not observe this phenomena.

The data, in Table5.4, are plotted out in Figure .It shows that adding rids is effective method, especially the porous flat is very thin, lower than 1.5mm. It means rid is the leading role in avoiding the broken. The porous flat takes the most load when its thickness is higher than 1.5mm. The dangerous load case is when the filter is doing back flush shown in Figure 5.8, which is coupled with the maximum principle stress distribution figures, Figure 5.6 and Figure 5.7. The allowable stress $[\sigma]$ for our filter is $32MPa$, so most of our cases will be broken when they work in the real life. There is a danger line drawn to help us estimate the performance of every case, and let us find out the start points based on strength safe in Figure 5.9. There are only three cases which are satisfy the strength design requirements, and all of these three cases have three rids. As shown in Figure 5.4, LMH is decreasing when the thickness is increasing. Case1.5_3 is the best case, because its porous flat is the final thin which give it a higher LMH compared with the other two cases.

5.5 CFD simulation for the best case

Based on the optimization theory and with the assist of ANSYS, the best start point Case1.5_3 which has 3 rids and its thickness is 1.5mm. For the detail of the boundary condition or some other thing else, please jump to B. Because the thickness

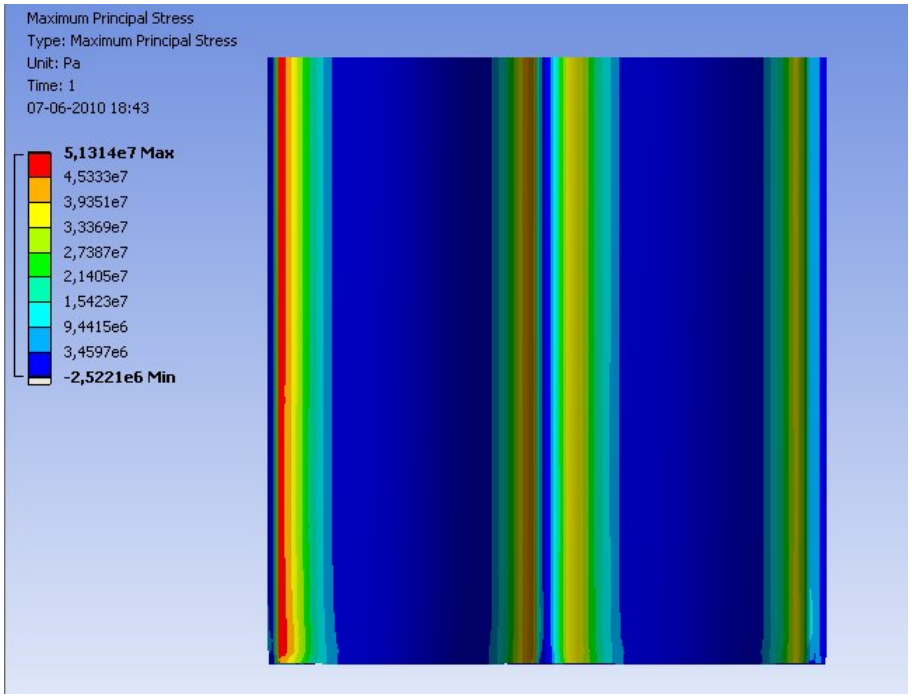

Figure 5.6: The pressure distribution of back flush

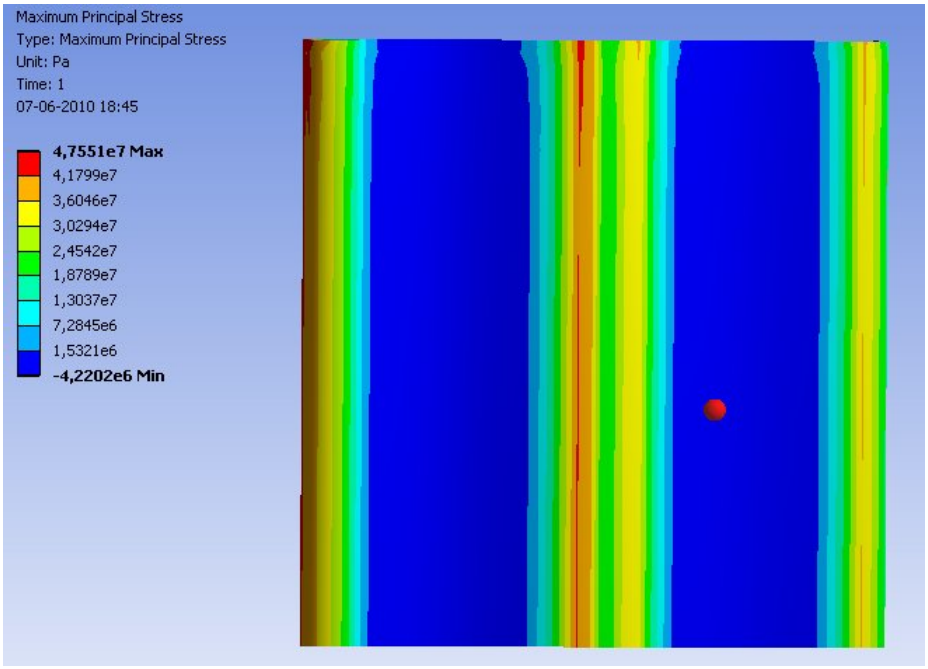

Figure 5.7: The pressure distribution of work state

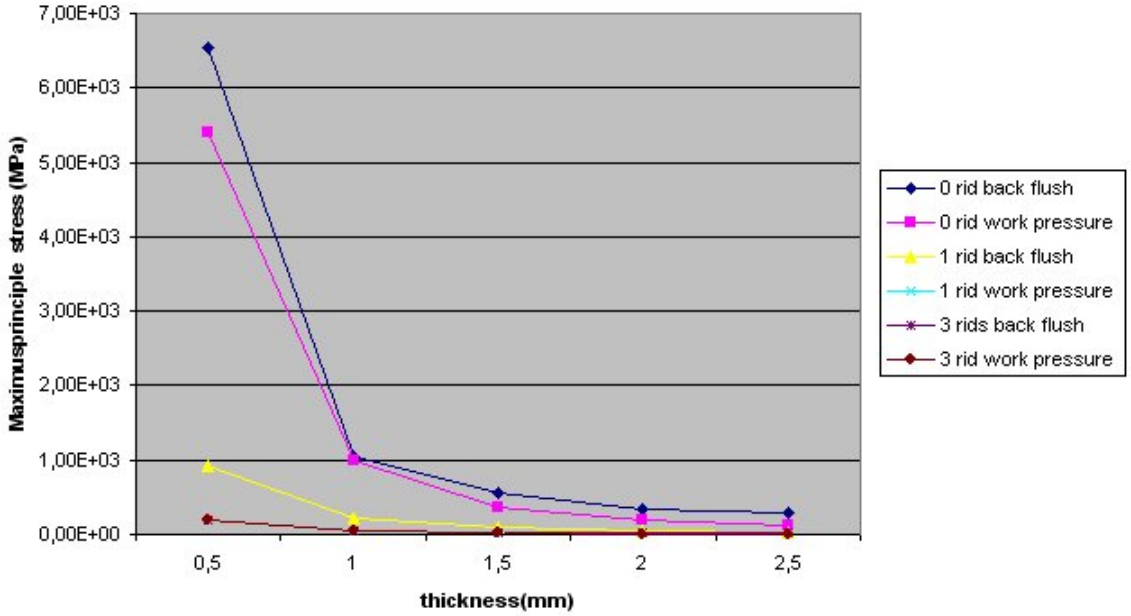

Figure 5.8: The relation between pressure and maximum principle stress

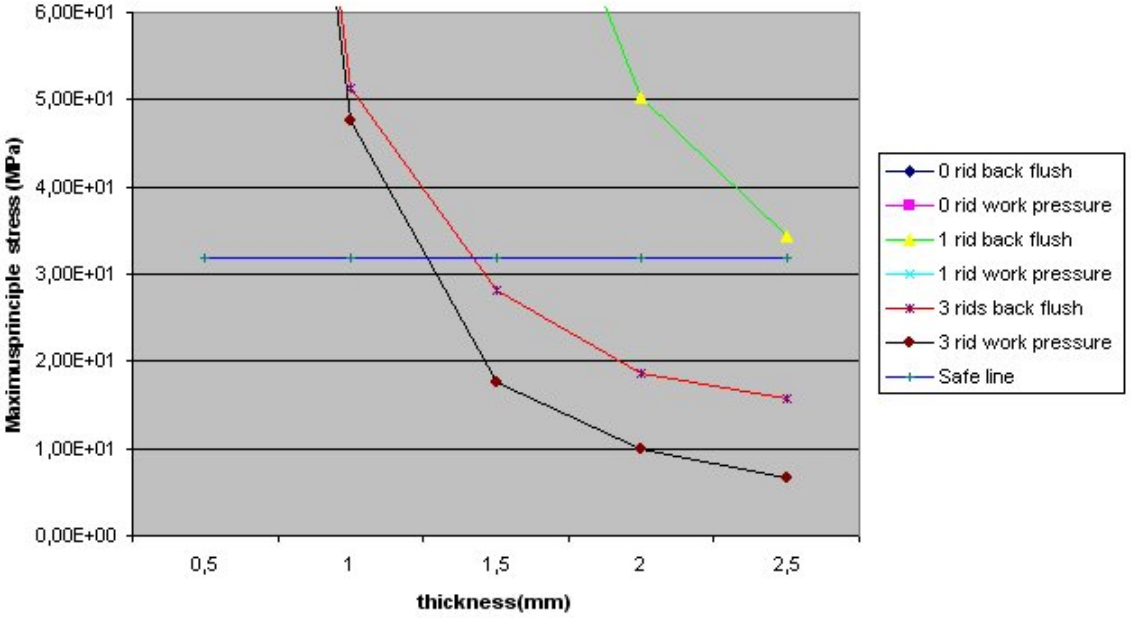

Figure 5.9: The detail of Figure 5.8

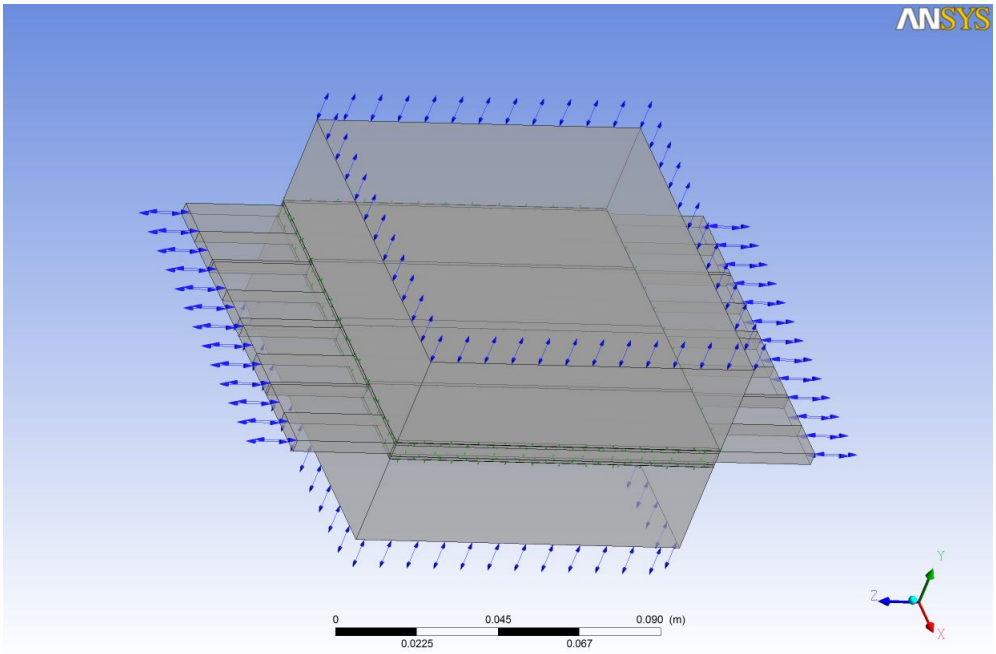

Figure 5.10: The picture of simplified CFD model

of membrane is ultranthin(0.085mm) compared with the thickness of core material part(1.5mm), especially compared with the length and the width of the cavity filter (100mm). And the membrane is surrounding the core_material, it is better to start the simulation at a sample case based on some assumption. As we talked in section 5.1, both the D area and C area can be recognized as flat in Figure 5.1. The geometry of filter is simplified as a porous hexahedron with four hexahedral channel through it(Figure 5.10). And the membrane domain is specified by two indemnifications for permeability and porosity. In this case, it can effectively decrease the RAM demand.

5.5.1 Result of CFD

The LMH and the pressure distribution, especially in the interface between the porous domain and the channel domain, are used to compared with the LMH, form hand calculation, and the pressure distribution on assumption. LMH can be easily gotten by expression and monitor. its value is 547 $l/h/m^2/bar$, compared the 520 $l/h/m^2/bar$,from Figure 5.4. The difference between results from simulation and hand calculation is 5.2%, this because both simulation and hand calculation are based on some assumptions, none of them can describe the real filter performance exactly. For this question, it will be improved in future by creating a correct filter geometry and linear equation in two unknowns to define different porous domains with different permeability and porosity.

The pressure in the channel is also important, because it is 0 Pa in the assumption. And whether there is some water flow out from the surfaces ,where are assumed as solid wall in the hand calculation, is another interesting point for this simulation. We just use a plane, transetting the porous plate and the clean water channel to get a rough view to check our assumption. most of the channel's pressure is under 10Pa.

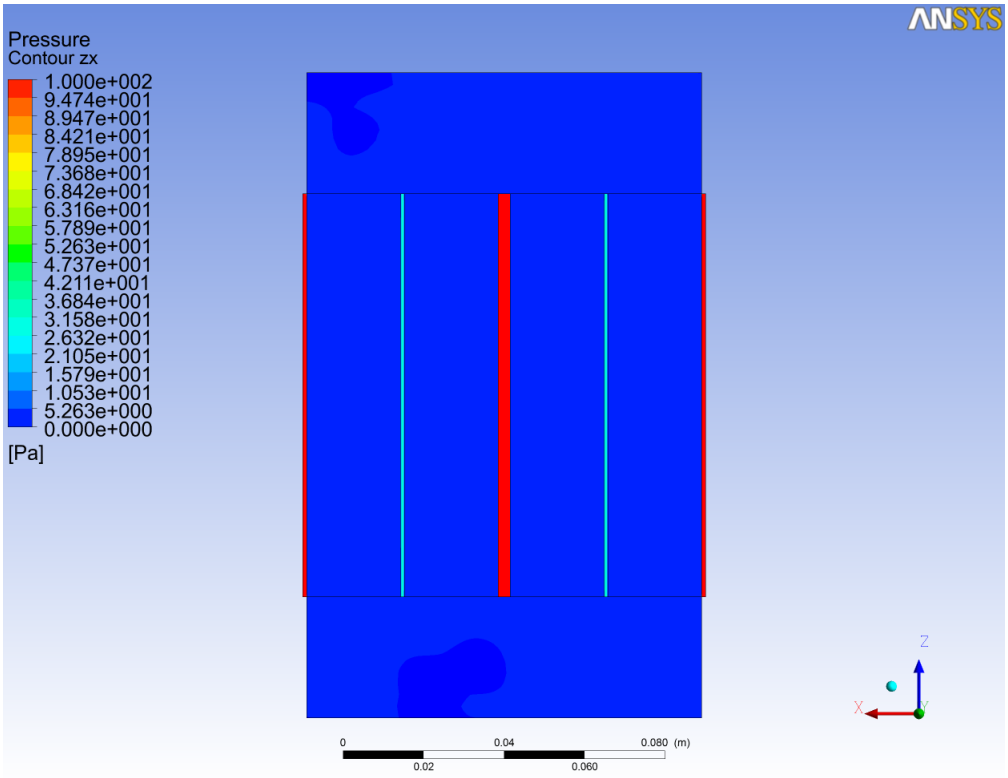

Figure 5.11: Pressure distribution in the xz plane of case1.5_3

from the pressure distribution in the xz plane in Figure 5.11. This negligible pressure difference between simulation and assumption is not worth mention compared with the pressure drop between inlet(2 bar) and the inner channels. There is some water flow out from the rid shown in Figure 5.12, the reason is that where the pressure difference is, where there is some permeat based on Darcy's Law[7, 4, 8].

5.6 On-going CFD

After we finished the Case1.5_3 simulation, we have found there are some flaws in our simulation, There geometry is not the real filter plate, and the porous domain should sink into fluid domain which means the porous domain-should be surrounded by the fluid domain. But as a sample for the future simulation, we just want use a simplest model which contains all the features of a filter, so Case1.5_1 is chosen as the example simulation in Figure 5.13. It is easy to see that the porous plate's permeable surface is totally sinked in the fluid domain, and the shape is imported from the Catia 3D geometry. And the functions for permeability and porosity (in C), cover the whole domain and describe the property fair enough. For the grid information and case set up, please refer to relevant appendix.

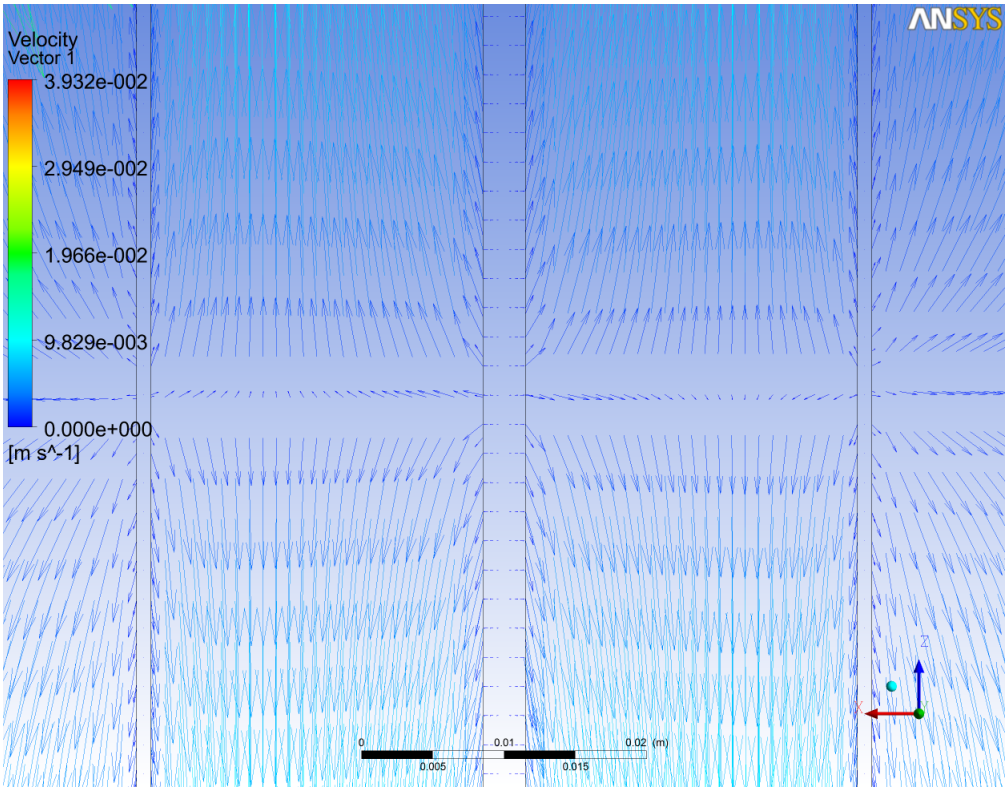

Figure 5.12: The vector in xz Plane

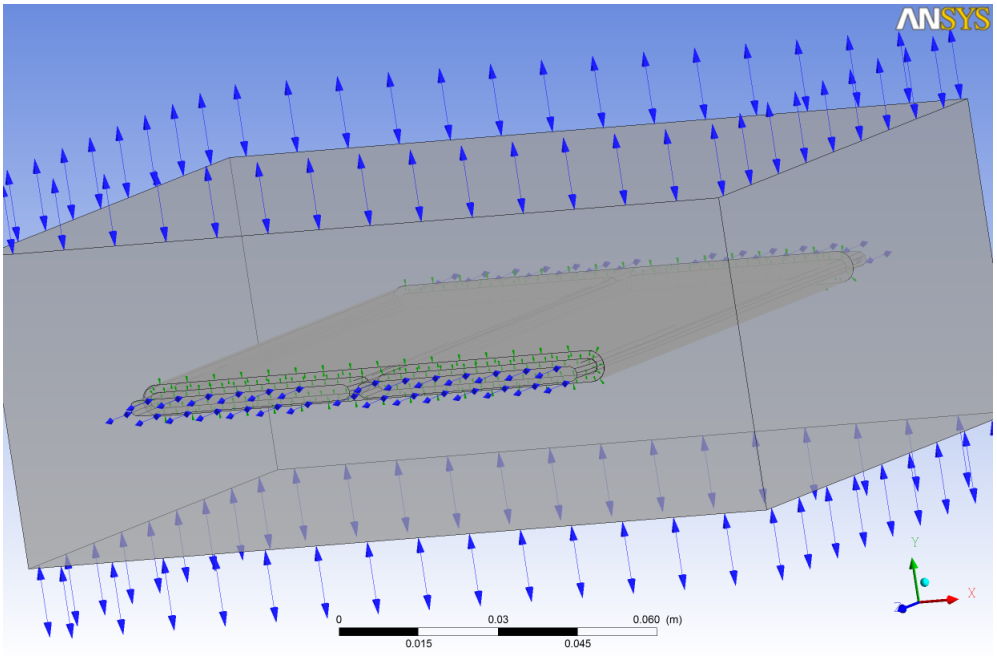

Figure 5.13: The schematic of On-going CFD

Conclusion and Outlook

Conclusion

The work present here can give a basic idea and knowledge to the people who just start the porous filter design for a filter-pump. And it also states the basic theory and considerations not only when we do some rough hand calculation but also when we set up simulations, both strength analysis and fluid simulation. In the CFD part, it also describes the topology strategy and give some ideas for specifying the special domains by step functions.

By the comparison between the hand calculation and the simulation, it makes sure that the hand calculation, coupled with simple strength simulation, it also gives some rough relationships among the thickness of porous plate and the number of rids, which can help us find a good start point when we try to set up the CFD simulation, plenty if time is not expended by this way.In the experiment part, it gives some function to get the LMH or permeability, especially for the oermeability of ultrathin membrane.

With this method to create cavity in side of the porous plate, the volume flwo rate of permeat can be increased to really higher level, and the pressure loss is reduced to acceptable level which is confirmed by the results of simulation.

Outlook

My simulation of the real geometry without any assunptions and defined by step functions has not start yet, which means the simulation modules need more improvement. And because of the leakage of computer programming, some of our optimum ideas can not transfer into practice software, but the concept of put all the parameters together is viable. I can not simulate the whole filter pump, even I have not transfer the knowledge from a ideal module to the real module, there is plenty of work need to do in my future job.

Bibliography

[1] GRIDPRO. *The AZ Graphic Manager Manual.* Program Development corporation, 300 Hamilton Ave, suite 409 White Plains, NY 10601, April 2000.

[2] Inc ANSYS. Cfx expression language.

[3] Shouxin Wang. *Enginnering Material Mechanics.* DLUT Publishing House, 2005.

[4] Jacob Bear. *Dynamics of Fluids in Porous Media.* Dover Publications, Inc, 1988.

[5] porvair filtration group. porvair introduction. http://www.porvairfiltration.com/news /highperformancefiltersforfueltank-inertingsystems.aspx.

[6] Wence Sun. *Enginnering Fluid Mechanics.* The publishing house of Dalian University of Technology, 2004.

[7] J.L.LAGE. *The Fundamental Theory of Flow through Permeable Media from Darcy To Turbulence.* PhD thesis, Mechanical Engineering Department, Southern Methodist University.

[8] D.A.NIE. *MODELLING FLUID FLOW IN SATURATED POROUS MEDIA AND AT INTERFACES.* PhD thesis, Department of Engineering Science, University of Auckland, Private Bag 92019, Auckland, New Zealand.

[9] Deling Shu. *The Performance of Engineering Material Mechnics.* Mechanical Industry Publishhouse, 2007.

[10] Kristoffer Gjendal and Henrik Bank Madsen. Flow in microporous cilicon carbide: an experimental and numerical study. Master's thesis, Technical University of Denmark, 2008.

[11] Department of Structural and Fluid Mechanics. *The Centrifugal Pump.* GRUNDFOS Management A/S Department of Structural and Fluid Mechanics, 2008.

[12] Jasbir S. Arora. *Introduction to optimum design.* McGraw Hill Book Co., 1989.

Appendix A

Ansys setip

The ansys setup in this report is just some basic skill, so the content of this appendix is an introdution or operational process:

A.1 Start static structural

After you start the Workbentch of ANSYS, the following step is: Toolbox ->Static structural (double click)

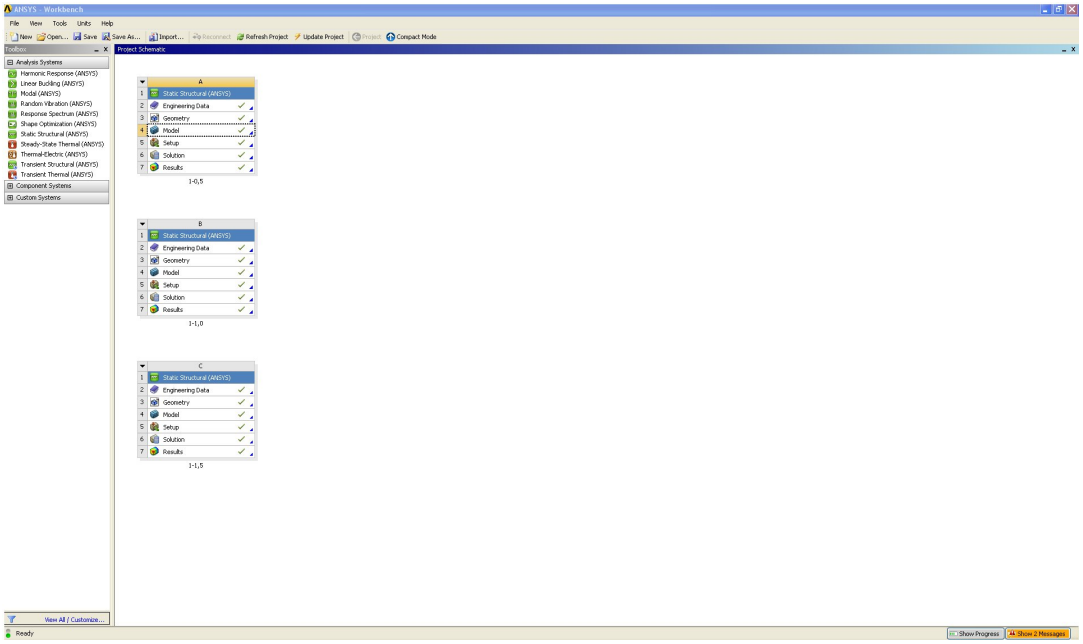

Figure A.1: Start static structural

A.2 Input the Enginnering Data

Double click the Enginnering Data bottom on one project tab, and then you will go into it, the only two datas need to change are Young's Modulus(4.6e+10Pa) and

Poisson's Ratio(0.24). Then click Return to Project, go back to the windows like Figure A.1.

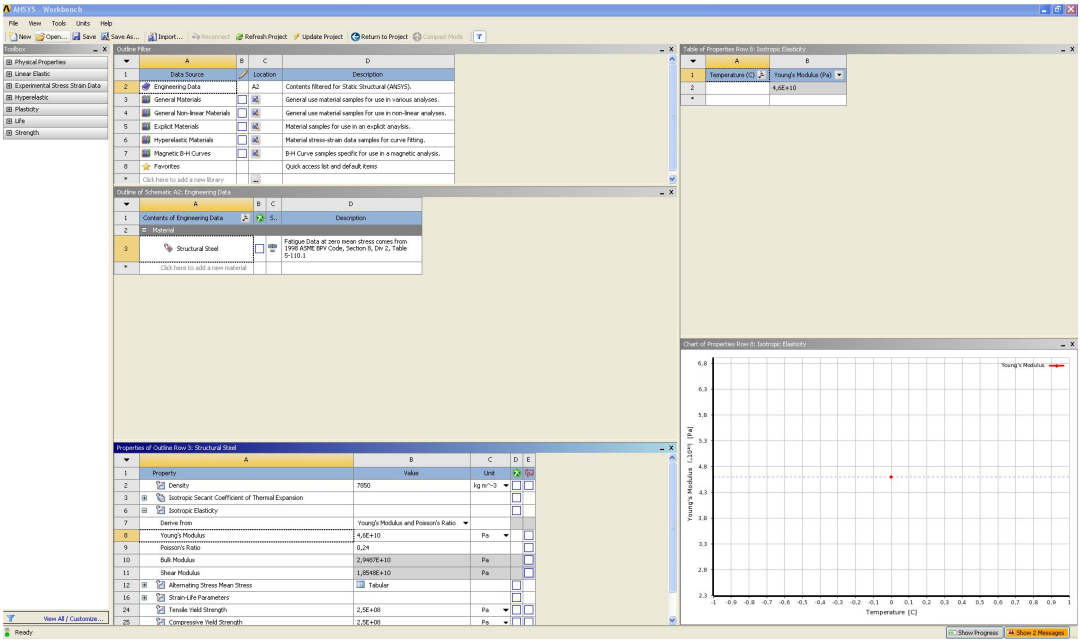

Figure A.2: engineering Data

A.3 Import the geometry

Right the bottom of 'Geomtry'(in Figure A.1) and chose 'Import', the go to the folder where your geometry file is.

A.4 Setup

Right click on the steup bottom (in Figure A.1) and click the red bottom Edit. then you will get into the. Just go through the outline, generate the mesh you want, set the pressure boundary condition and the frictionless support, chose the solution you want. After all the steps are ok, right click solution, then click run.

After its computing, click the result you want to check.

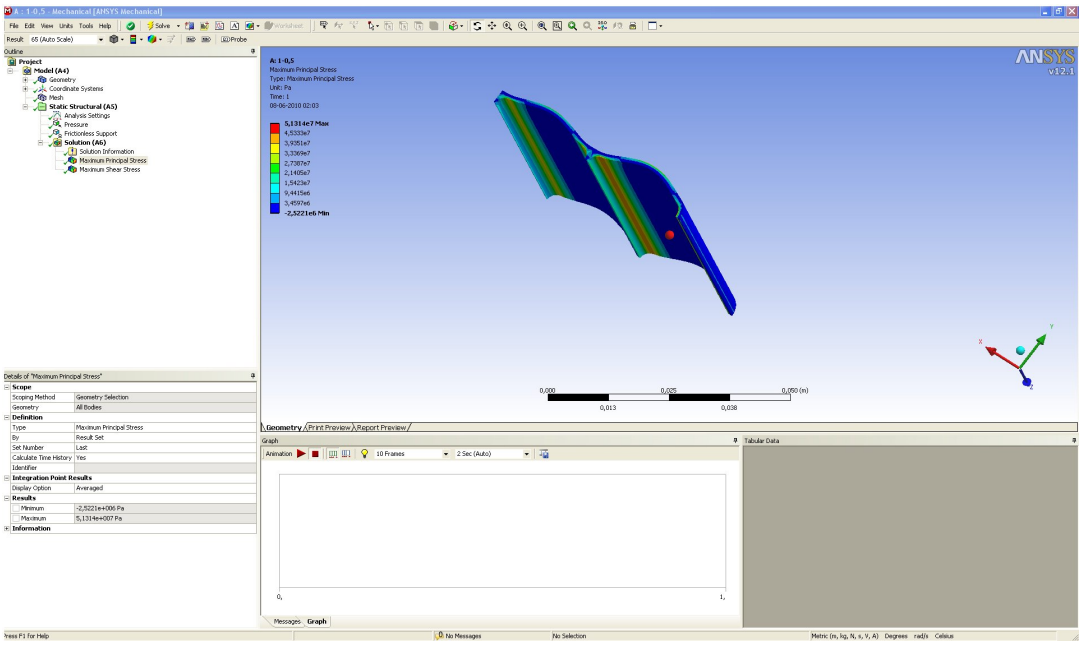

Figure A.3: Mechnical Tab

Appendix B

Topology strategy based on GridPro Manual1

For the topology, we want to have a comparsion among the last three grids for porous plate.The most important step is creat topo in one of its cross section, the topo for the other side can just copy it from what we have done in the first cross section. The quality of the topology on the cross section is the determinant for the quality of the whole porous plate and the degree of simulation's accurancy. After the introduction of these three topology, there is ancomparsion about skewness(Norm Volume), warpage and the number of cells.

B.1 The first grid

Because we want to define the membrane by using step-function, so we have not specified the interface between core and membrane as the top on in Figure B.1, and the topology is shown below in Figure B.1. After copying this topology to the other side and setting a series of density, then we get the grid shown in Figure B.2. The density near the outer surface is set by clu command.

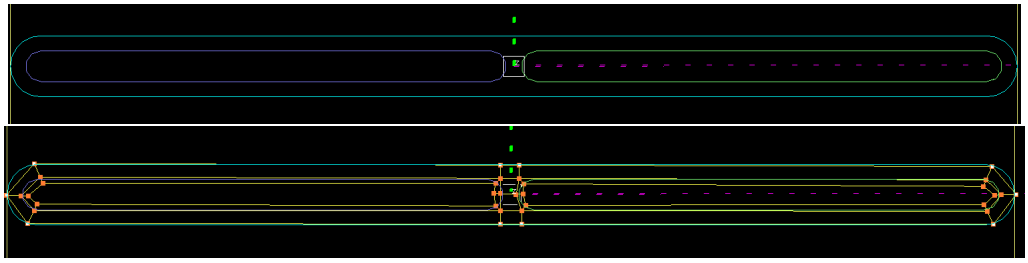

Figure B.1: First topology

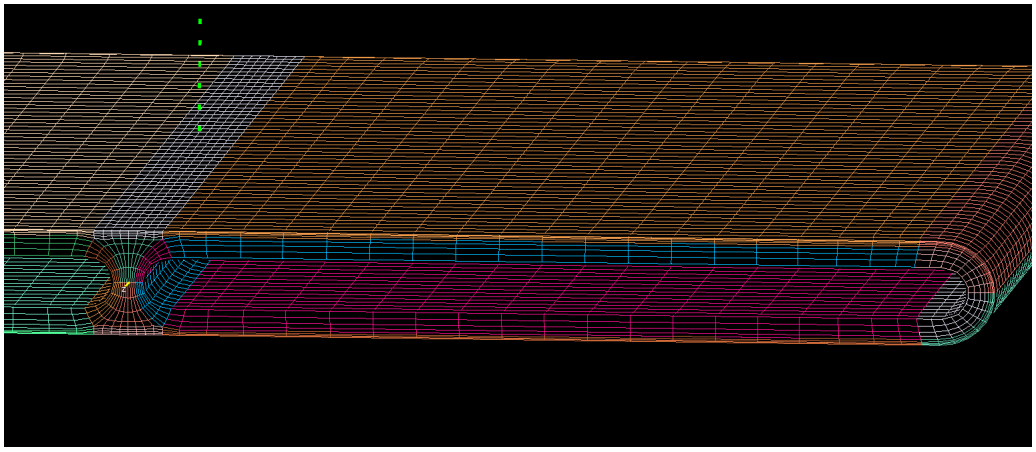

Figure B.2: Detial of First Grid

B.2 The second grid

In order to improve teh quality of the grid and get information from the interface in the CFX-Post, the interface between membrane and core has been added and the new topology is mostly the same as the first one, just insert a line near the interface shown in Figure B.3.In the second topology, the density in the membrane domain can be set directly. Then we get grid shown in Figure.

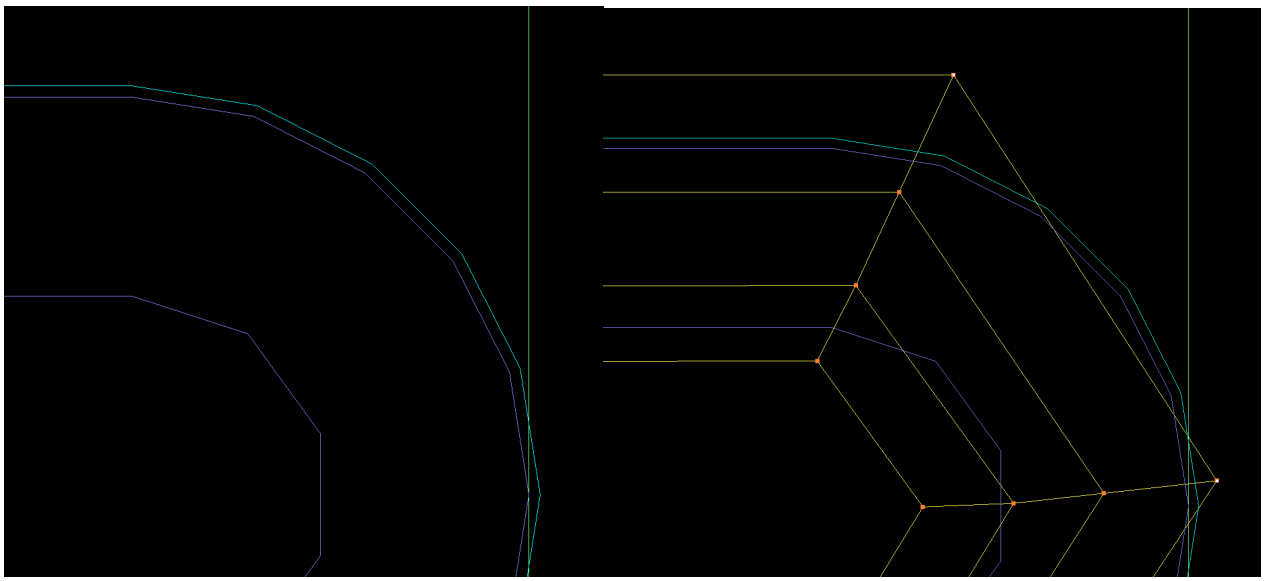

Figure B.3: Second topology and surfaces

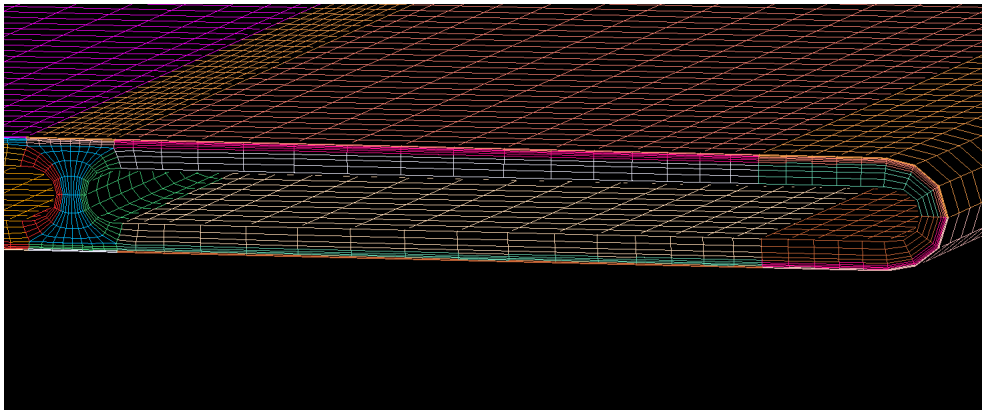

Figure B.4: The second grid

B.3 Comparison

The skewness, warpage and the number of cells are whoen in Table B.1. Skewness is the higher the better, and it should not be lower than 0.05. Warpage should no higher than 75 degree (GridPro User Manual) . It is obvious that the quality of the first one si better than the second one, but the second one has an interface could be used to catch datas, and the first one's mesh can not divided into membran domain and core domain exactly compared with the second one. In this report, the second one is recognized as the better on, and will be used in following up simulations.

	Skewness	Warpage(degree)	Cells
First	0.52	4.76	51200
Second	0.49	6.00	64800

Table B.1: Datas of Grids

Appendix C

Step Functions for CFD simulation2

Because of the thickness of membrane, attached to the outer surface of core_material(in Figure. C.1), is just 0.085mm,which is extremely small compared withe the size of the filter. It is not viable to creat its geometry and mesh it independently, but the permeability and porosity of this membran should be defined. Expression, in CFX, is a suitable solution to do so. It can give the differnet physical paramters to different parts of one geometry.

Before we start our formulations of the permeability and porosity, it is very important to know the distribution of differnent paramters in this geometry, because the geometry of this cross section is symmetrical, the small picture(in Figure C.1 and Figure C.2) is used to give the detail to you. Based on these two figures and to make the setp function be easily understood, this filter will be divided into seven areas. And all of our formulation is based on the 1_1.5 filter, there is one channel in this filter and the thickness of this filter is 1.5mm.

TM is used to stand for the top of membrane, BTM is used stand for the bottom of membrane, LM is the left of membrane and RM is the right of membrane. For core_material. C is the main boday, LC is its left and RC isits right. The field of definitions is shown in Table C.1. The rile for step function is easy to understand, the TM is used as an example to describe the rule:

In the step fucntion, all the values in the parentheses must be constant without unit. If the value is positive number, otherwise it is 0. Because in the x-direction $-47 \leq x \leq 47$, so we need step function do twice judges. For $-47 \leq x$, it should be step(x/1[m]-(-47e-3)), for $x \leq 47$ it should be step(47e-3-x/1[m]). If x in the range from -47mm to 47mm, it should keep both step(x/1[m]-(-47e-3)) and step(47e-3-x/1[m]) equal to 1, then step(x/1[m]-(-47e-3))*step(47e-3-x/1[m]), for the rest could be find in Table C.2 and Table C.3. We just finish the logic of field of definitions, the next step is give the value to them:

$$step(y/1[m] - (3e-3)) * step(3.085e-3-y/1[m]step(y/1[m] - (3e-3))$$

$$* step(3.085e-3-y/1[m]) * 1.489e-16[m^2] \quad \text{(C.1)}$$

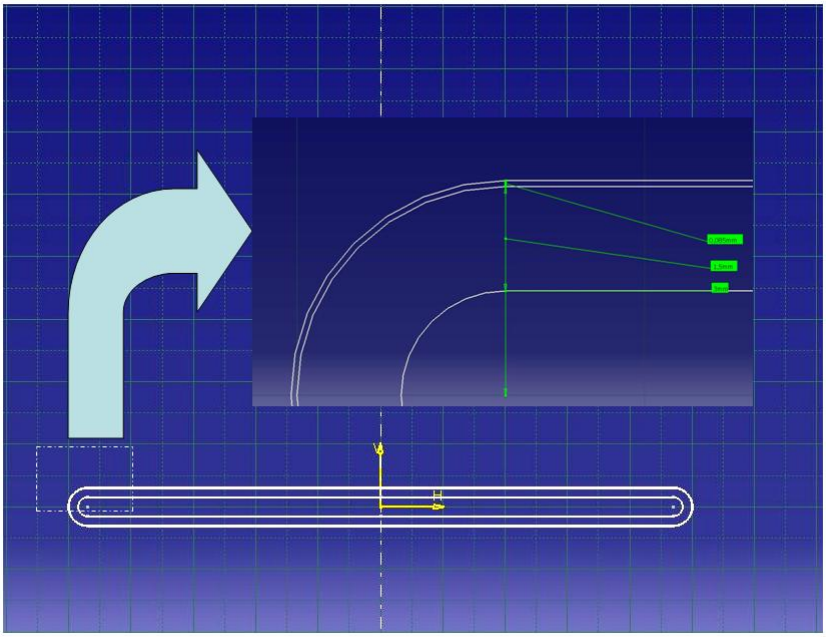

Figure C.1: Cross Section of 1_1.5 Filter

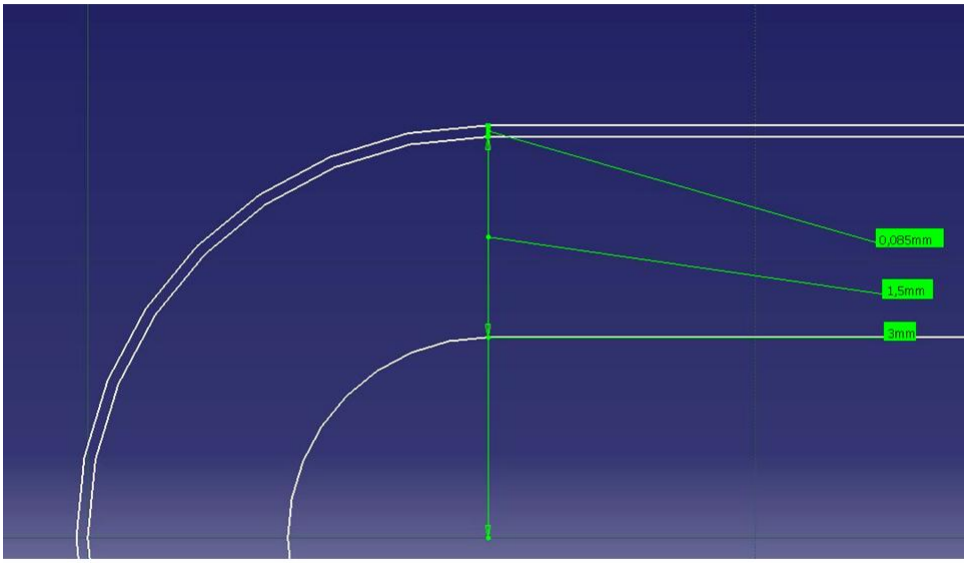

Figure C.2: Detail of the filter membrane

Fileds	x-direction(mm)	y-direction(mm)
TM	$-47 \leq x \leq 47$	$3 \leq y \leq 3.085$
BTM	$-47 \leq x \leq 47$	$-3.085 \leq y \leq -3$
LM	$-50.085 \leq x \leq -50$	$3^2 \leq (x^2 + y^2) \leq 3.085^2$
RM	$50 \leq x \leq 50.085$	$3^2 \leq (x^2 + y^2) \leq 3.085^2$
C	$-47 \leq x \leq 47$	$-3 \leq y \leq 3$
LC	$-50 \leq x \leq -47$	$0 \leq (x^2 + y^2) \leq 3^2$
RC	$47 \leq x \leq 50$	$0 \leq (x^2 + y^2) \leq 3^2$

Table C.1: Field of definitions

Fileds	Step(x)
TM	step(x/1[m]-(-47e-3))*step(47e-3-x/1[m])
BTM	step(x/1[m]-(-47e-3))*step(47e-3-x/1[m])
LM	step(x/1[m]-(-50.085e-3))*step(-50e-3-x/1[m])
RM	step(x/1[m]-(50e-3))*step(50.085e-3-x/1[m])
C	step(x/1[m]-(-47e-3))*step(47e-3-x/1[m])
LC	step(x/1[m]-(-50e-3))*step(-47e-3-x/1[m])
RC	step(x/1[m]-(47e-3))*step(50e-3-x/1[m])

Table C.2: Step function for every field of definitions in x direction

Now we have finished one field's definition, the rest can be gotten by the same way. After that, all the equation should be connected by plus +, because the limit of setting type, the full expression is not shown here, but you can find it in the DVD attached to this report.

Fileds	Step(y)
TM	step(y/1[m]-(3e-3))*step(3.085e-3-y/1[m]
BTM	step(y/1[m]-(-3.085e-3))*step(-3e-3-y/1[m]
LM	step((3.085e-3)^2-((x+47e-3[m])^2+y^2)/1[m^2])
	*step((x+47e-3[m])^2+y^2)/1[m^2]-(3*1e-3)^2)
RM	step((3.085e-3)^2-((x-47e-3[m])^2+y^2)/1[m^2])
	*step((x-47e-3[m])^2+y^2)/1[m^2]-(3*1e-3)^2)
C	step(y/1[m]-(-3e-3))*step(3e-3-y/1[m]
LC	step((3e-3)^2-((x+47e-3[m])^2+y^2)/1[m^2])
RC	step((3e-3)^2-((x-47e-3[m])^2+y^2)/1[m^2])

Table C.3: Step function for every field of definitions in y direction

Appendix D

Porosity measurement

D.1 Porosity Measurement

Porosity (n), or volumetric porosity, is a property of medium and it is defined as the ratio of void space's volume (U_v) to the porous medium's bulk volume (U_b)[4]:

$$n = \frac{U_v}{U_b} = \frac{U_b - U_s}{U_b} \tag{D.1}$$

Where U_s is the volume of the solid within U_b.The importance of both of them for fluid dynamics. Here I also want to give a special explanation. U_s is not only the volume of the absolute solid but also contains the volume of the pore space which is not interconnected with the others. Even some special pore space connect with the others, deed-end pore (fig. D.1) or stagnant pocket, is also should be recognoized as a part of U_b. In this ropeot, unless otherwise specified, the volume of solid (U_s) is refered to the noeffictive volume and the void space (U_v) is effective space.So the porosity here is the effective porosity.

D.2 Porosity Measurement

A lot of metods are practiced for determining porosity. From the porosity definition, it is obvious that every method needs to get two of those three volumemes: the pore volume (U_v) of the sample, the volume of its solid martrix (U_s) and its bulk or total volume (U_b). These methods based on such volume determinations,cakked direct methods, the differences of them is the ways they get the volumes and which two they try to get.

As a matter of convenience, it is better to chose a sample with a well defined geometric shape and measure its dimensions. In my project, the sample's shape is a rectangular block. Hereby, the direct method described in my project is based on Boyle-Mariotte's law[4]: U_b is determined by a compression chamber. Several equipments are convenient, all of these methods are also based on the Boyle-Mariotte gas low. Practically, two chambers are connected with each other by a valve (fig. D.2). The sample is put into the firet chamber (volume U_1) and its pressure is p_1. The other chamber, whose volume is U_2, is initially evacuated of gas. The gas in the first chamber will isothermically diffuse into the second chamber when the valve,

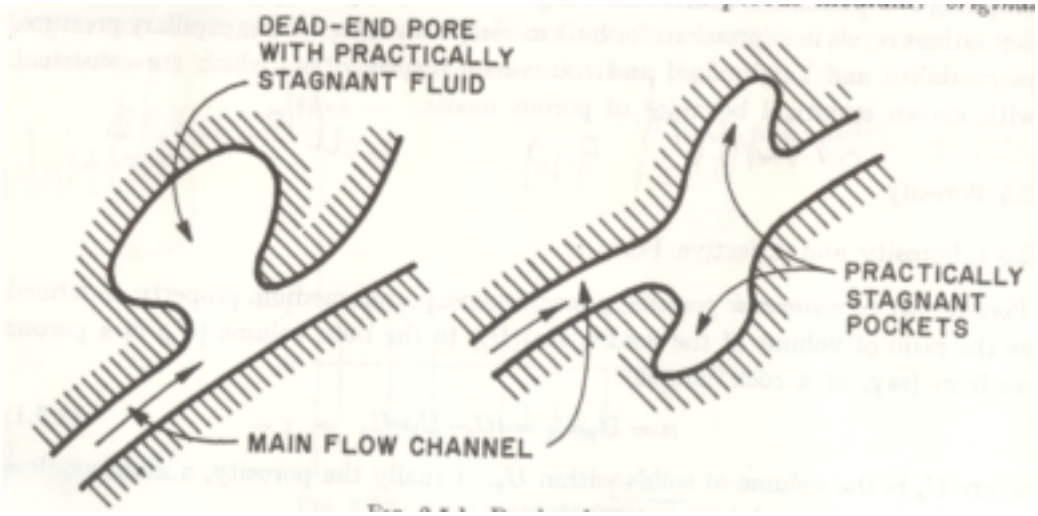

Figure D.1: Dead-end pores.[4]

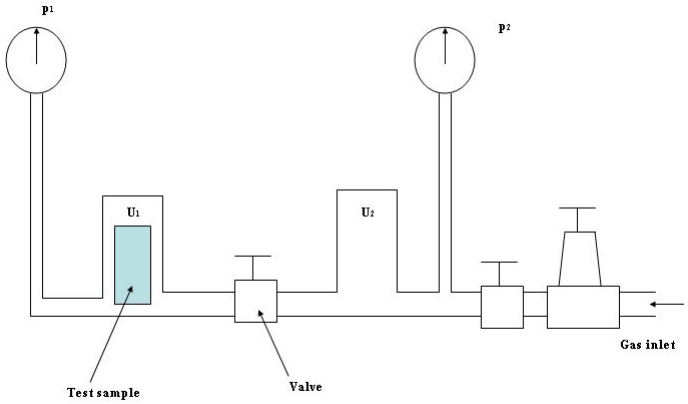

Figure D.2: Porosimeter based on Boyle Mariotte's law

between two chambers, is opened. The pressure, when the pressure is constant, is registered by p_2. We have:

$$(U_1 - U_s)p_1 = (U_1 - U_s + U_2)p_2 \tag{D.2}$$

or:

$$U_s = U_1 - \frac{p_2}{p_1 - p_2}U_2 \tag{D.3}$$

Then we can get the porosity:

$$n = \frac{U_b - U_s}{U_b} = \frac{U_b - (U_1 - \frac{p_2}{p_1 - p_2}U_2)}{U_b} \tag{D.4}$$